Marine Chemistry 211 (2019) 117–130

Contents lists available at ScienceDirect

Marine Chemistry

journal homepage: www.elsevier.com/locate/marchem

REE distribution and Nd isotope composition of estuarine waters and bulk sediment leachates tracing lithogenic inputs in eastern Canada

Marie Casse[a,b,1], Jean-Carlos Montero-Serrano[a,b,*,1], Guillaume St-Onge[a,b], André Poirier[b]

[a] Institut des sciences de la mer de Rimouski, Canada Research Chair in Marine Geology, Université du Québec à Rimouski, 310 allée des Ursulines, Rimouski, Québec G5L 3A1, Canada

[b] GEOTOP Research Center, 201 Av. Président Kennedy, Montréal, Québec, H2X 3Y7, Canada

ARTICLE INFO

Keywords:
Estuary and gulf of St. Lawrence
Rare earth element
Neodymium isotopes
Strontium isotopes
Particle scavenging
Sediment provenance
Estuarine processes

ABSTRACT

The rare earth element (REE) concentrations and the neodymium (Nd) and strontium (Sr) isotope compositions of the detrital fraction and authigenic Fe–Mn oxyhydroxide coatings of marine sediments may provide valuable information for better understanding the pathways of weathering inputs and estuarine and coastal exchange processes on different time scales. Here, we present the REE concentrations and $^{143}Nd/^{144}Nd$ (expressed in epsilon units, εNd) and $^{87}Sr/^{86}Sr$ ratios of detrital and authigenic (leached Fe–Mn oxyhydroxides) fractions from sediment core-top samples and of estuarine water samples collected in the Estuary and Gulf of St. Lawrence (EGSL) and continental shelf off southeastern Canada. The REE distribution patterns, εNd values, and $^{87}Sr/^{86}Sr$ isotopic values from the detrital fraction allow for the discrimination of sediment from continental sources in the EGSL. Sediments in the Baie des Chaleurs and on the continental shelf, which have εNd values ranging from −14.3 to −16, $^{87}Sr/^{86}Sr$ values ranging from 0.72708 to 0.71475, and low La/Yb and Gd/Yb ratios, are mainly supplied by the early Paleozoic Appalachian Mountains. In contrast, sediments in the Laurentian and Esquiman channels (εNd = −18.7 to −21.8, $^{87}Sr/^{86}Sr$ = 0.72068 to 0.72607, and high La/Yb and Gd/Yb ratios) come from the Grenvillian metamorphic rocks in the Canadian Shield, and surface sediments on the southern Labrador Shelf (εNd = −28.7, $^{87}Sr/^{86}Sr$ = 0.73062, and high La/Yb and Gd/Yb ratios) mainly originate from the Hudson Strait and Baffin Bay. The εNd values obtained from estuarine water samples and bulk sediment leachates are unradiogenic, with values ranging between −18.9 and − 21.7 and between −16.1 and − 27.2, respectively. Based on these results and the dissolved REE concentrations, we speculate that salt-induced coagulation of colloidal matter, dissolution of lithogenic sediments from the adjacent continents (notably from the erosion of the Grenville Province on the North Shore), bottom scavenging within the nepheloid layer, and brine rejection during sea ice formation significantly influence the distribution of REEs and the authigenic εNd signal throughout the water column in the EGSL. Overall, our results both underscore the fact that caution must be exercised when interpreting authigenic εNd records due to bottom water-mass mixing in estuarine and coastal marine environments and highlight the potential of REE and Nd–Sr isotope compositions in investigating changes in sediment sources and transport pathways in the EGSL.

1. Introduction

Estuaries are the interface between rivers and the ocean, and in these environments, the distribution of dissolved and particulate trace elements, including rare earth elements (REEs), depends not only on the chemical composition of the source rocks (Taylor and McLennan, 1985) but also on the physical and chemical processes that take place within the estuary (e.g., Palmer and Elderfield, 1985; Goldstein and Jacobsen, 1988; Elderfield et al., 1990; Sholkovitz, 1993, 1995; Adebayo et al., 2018). Therefore, estuaries significantly influence the trace element input from rivers into coastal waters and ultimately into the open ocean (Pourret and Tuduri, 2017). Due to their high charge and small ionic radius, dissolved REEs are particle-reactive elements that are efficiently removed in the estuarine zone (Sholkovitz, 1993, 1995; Rousseau et al., 2015). Much of the removal of REEs, in particular light REEs (LREEs; such as La and Nd), in river-estuarine systems occurs at low salinities

* Corresponding author at: Institut des sciences de la mer de Rimouski, Canada Research Chair in Marine Geology, Université du Québec à Rimouski, 310 allée des Ursulines, Rimouski, Québec G5L 3A1, Canada.
E-mail address: jeancarlos_monteroserrano@uqar.ca (J.-C. Montero-Serrano).
[1] Authors contributed equally.

https://doi.org/10.1016/j.marchem.2019.03.012
Received 18 September 2018; Received in revised form 14 March 2019; Accepted 16 March 2019
Available online 18 March 2019
0304-4203/

(< 6.6), reflecting REE scavenging by salt-induced coagulation of river-borne colloids and adsorption onto Fe-organic colloids and particulate organic carbon (Elderfield et al., 1990; Goldstein and Jacobsen, 1988; Sholkovitz, 1993, 1995; Sholkovitz and Szymczak, 2000; Rousseau et al., 2015; Merschel et al., 2017).

Among the REEs, neodymium (Nd) isotopes (denoted εNd, which reflects the $^{143}Nd/^{144}Nd$ ratio normalized to the chondritic uniform reservoir; Jacobsen and Wasserburg, 1980) are a sensitive tracer for water mass mixing in the open ocean given the Nd residence time in seawater on the order of 500–1000 years (Tachikawa, 2003) and the distinct dissolved Nd isotope compositions of the major water masses involved (e.g., Frank, 2002; Goldstein and Hemming, 2003; Jeandel et al., 2007; Lacan et al., 2012). Seawater displays regional εNd signatures derived primarily from riverine continental input, particle-dissolved exchange processes (a process commonly referred to as boundary exchange) and/or benthic Nd flux (e.g., Frank, 2002; Jeandel et al., 2007; Wilson et al., 2013; Jeandel, 2016; Abbott et al., 2016; Haley et al., 2017). It is possible to reconstruct past deep-water Nd isotope signatures in seawater by analyzing the authigenic fraction from marine sediments, such as ferromanganese (Fe–Mn) oxyhydroxide coatings (e.g., Rutberg et al., 2000; Piotrowski et al., 2004; Bayon et al., 2004; Gutjahr et al., 2007). The Nd isotope signatures from authigenic iron (Fe) and manganese (Mn) coatings directly reflect the composition of the seawater because dissolved trace elements are incorporated by coprecipitation processes during early burial in the top few centimeters of sediments (e.g., Haley et al., 2004; Gutjahr et al., 2007). Thus, it has been assumed that bottom-water Nd isotope signatures are equivalent to those obtained from sediment pore water in the upper few centimeters (Abbott et al., 2016; Haley et al., 2017). Under oxic to suboxic conditions, strontium (Sr) is also incorporated into Fe–Mn oxyhydroxide coatings within the uppermost few centimeters of the seafloor (Haley et al., 2004). The oceanic residence time of Sr in the water column (2.5 Ma) is much longer (Hodell et al., 1990) than the global turnover time of the ocean (approximately 1500 yr; Broecker and Peng, 1982). Consequently, the Sr isotope ratio of seawater has changed but is globally homogeneous at any given time (with a modern value of $^{87}Sr/^{86}Sr = 0.70917$; Palmer and Elderfield, 1985; Henderson et al., 1994; El Meknassi et al., 2018). Thus, the Sr isotope signals obtained from authigenic Fe–Mn oxyhydroxide coatings can help to assess the presence or absence of detrital contributions in bulk sediment leachates (e.g., Gutjahr et al., 2007; Molina-Kescher et al., 2014). Moreover, lithogenic Sr is very mobile during chemical weathering and can be easily removed from continental source regions (e.g., Millot et al., 2002; Stevenson et al., 2018). Consequently, variations in the $^{87}Sr/^{86}Sr$ ratio of detrital sediments have been shown to be a powerful tool for identifying changes in continental weathering regimes on different time scales (e.g., Frank, 2002; Meyer et al., 2011). Therefore, the combined use of εNd and $^{87}Sr/^{86}Sr$ values from detrital sediment may help in the investigation of changes in weathering regimes and sediment provenance over time (e.g., Meyer et al., 2011; Asahara et al., 2012; Molina-Kescher et al., 2014).

The Estuary and Gulf of St. Lawrence (EGSL) in eastern Canada (Fig. 1) includes very dynamic environments from a sedimentary and geochemical point of view. Indeed, the EGSL is characterized by a large volume of continental runoff, strong stratification of water masses (Koutitonsky and Bugden, 1991), seasonal sea ice cover (Galbraith et al., 2016), and high modern sedimentation rates (up to 0.74 cm/yr; Smith and Schafer, 1999; St-Onge et al., 2003; Thibodeau et al., 2013). However, the origin, mixing and propagation of detrital sediments and the influence of the input of riverine particulate material on estuarine water chemistry in the EGSL have been poorly documented (e.g., D'Anglejan and Smith, 1973; Yeats and Loring, 1991; Casse et al., 2017). Thus, assessment of the REE concentrations and Nd and Sr isotope compositions of marine sediments and estuarine waters from the EGSL may provide valuable information to better understand the sedimentary dynamics and estuarine exchange processes occurring within this cold temperate region.

In this context, we present new REE concentrations and Nd and Sr isotope compositions for detrital and authigenic (leached Fe–Mn oxyhydroxides) fractions from sediment core-tops and for estuarine water samples collected in the EGSL and continental shelf off southeastern Canada. These data were used to (1) identify different source areas and transport pathways of detrital material in eastern Canada, (2) assess the presence or absence of detrital contributions in the REE and Nd isotope signatures extracted from the bulk sediment leachates (authigenic signal), and (3) assess the potential influences of estuarine processes and the input of lithogenic riverine materials on the dissolved REE and εNd patterns of estuarine waters in the EGSL.

2. Environmental setting

2.1. Regional morphology and geological setting

The EGSL bathymetry is profoundly marked by the Laurentian Channel, a U-shaped submarine valley resulting from Quaternary glacial erosion (Piper et al., 1990; St-Onge et al., 2011). This dominant topographic feature (250–500 m deep) extends from the eastern Canadian continental shelf to the mouth of the Saguenay Fjord near Tadoussac (e.g., St-Onge et al., 2011). Two other U-shaped channels are also well defined in the northeastern gulf: the Anticosti and Esquiman channels (Fig. 1B). Moreover, surface sediments in the EGSL are characterized by fine-grained sediments (notably fine silts) in the deep central parts of the Laurentian Channel and by coarser-grained sediments (gravel, sand and, in lesser proportions, fine silt) in the slopes and adjacent shelves (Loring and Nota, 1973; St-Onge et al., 2003; Barletta et al., 2010; Pinet et al., 2011; Jaegle, 2015).

Two main geological provinces characterize southeastern Canada (Fig. 1A): (1) the Canadian Shield in the northern part, typified by old silicate rocks (Paleo- to Mesoproterozoic granites and gneisses) from the Grenville and Makkovik provinces (Culshaw et al., 2000; Farmer et al., 2003), and (2) the Appalachian Province in the southern part, composed of Paleozoic sedimentary rocks (including shale, limestone, dolostone, and calcareous shale; Loring and Nota, 1973). In this latter province, Paleozoic carbonate rocks crop out mainly on Anticosti Island and the western Newfoundland coast (Loring and Nota, 1973; Ebbestad and Tapanila, 2005).

According to several mineralogical and geochemical studies from eastern Canada (e.g., Loring and Nota, 1973; Farmer et al., 2003; Jaegle, 2015; Casse et al., 2017), detrital sediments in the Gulf of St. Lawrence are mainly derived from the eastern part of the Appalachians (notably from the Canadian Maritime Provinces) and western Newfoundland coast, with the Grenvillian metamorphic rocks of the Canadian Shield on the North Shore being a secondary source. Conversely, in the lower St. Lawrence Estuary, detrital sediments mainly originate from the North Shore (Jaegle, 2015; Casse et al., 2017). Sedimentary inputs from the southern Labrador margin are derived mainly from the Grenville and Makkovic provinces as well as from the Hudson Strait and Baffin Bay (Farmer et al., 2003).

2.2. Hydrological setting

The eastern Canadian continental shelf is directly affected by the southward flow of the Labrador Current Water (LCW), a shelf-bathing water mass that reaches depths slightly > 600 m (Yashayaev et al., 2007). The LCW can be divided into 2 major branches (Fig. 1A), outer and inner (Lazier and Wright, 1993; Yashayaev et al., 2007). The outer LCW is composed of the West Greenland Current (WGC) and the Baffin Current (BC) and carries approximately 80% of the south-bound water, while the inner LCW is strongly influenced by outflow from the Hudson Strait that mixes with Baffin Bay water (Drinkwater, 1996; Lazier and Wright, 1993).

The EGSL is a transitional environment between the St. Lawrence

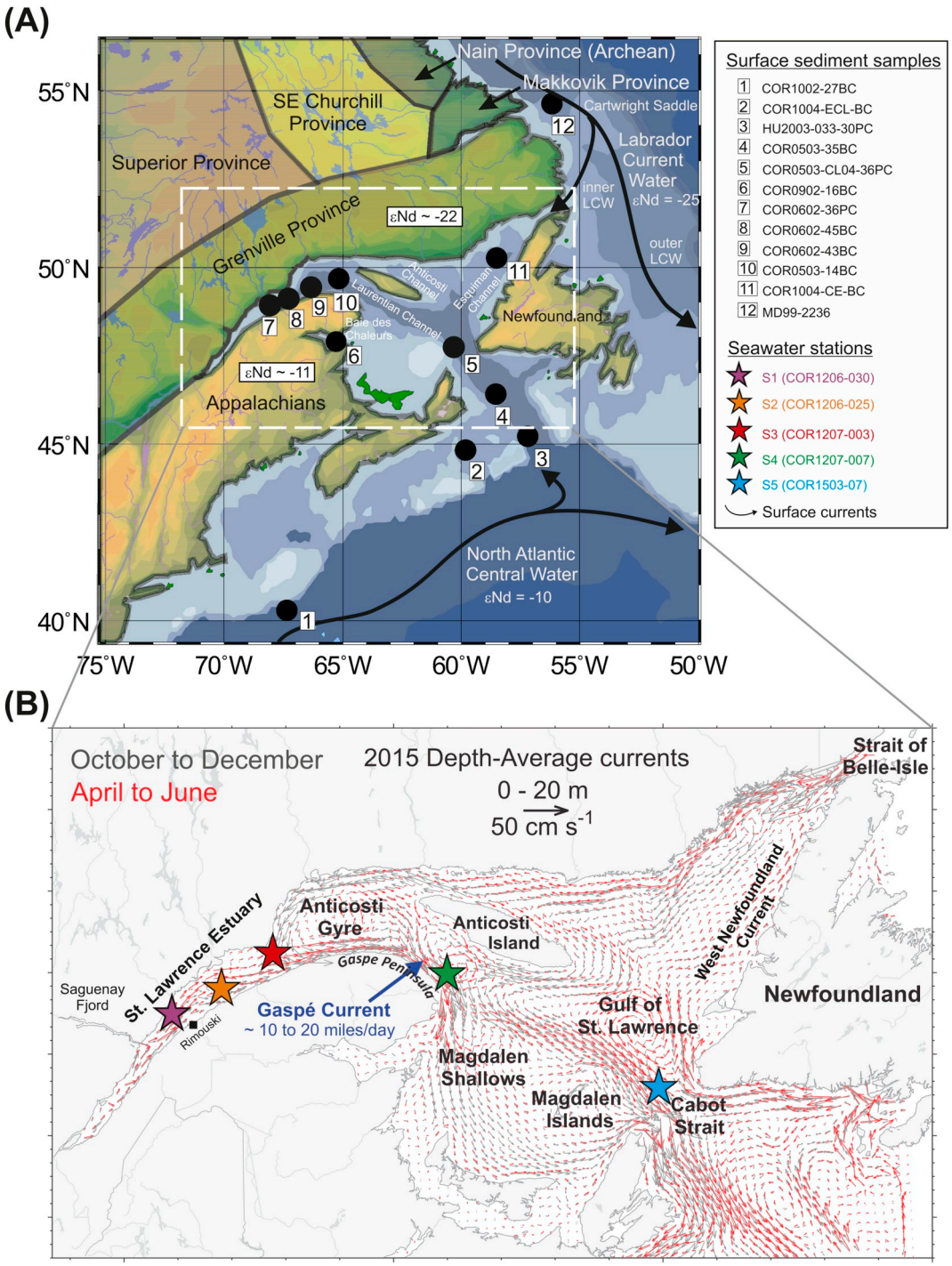

Fig. 1. (A) General map of the EGSL representing the location of the different core-top sediments analyzed in this study. The continental geological provinces are illustrated according to Farmer et al. (2003) with the εNd values of the Labrador Current Water (εNd ≈ −25; Piepgras and Wasserburg, 1987; Filippova et al., 2017) and North Atlantic Current Water (εNd ≈ −10; Spivack and Wasserburg, 1988; Lacan et al., 2012). (B) Simplified surface circulation models from the EGSL (modified from Galbraith et al., 2016) from October to December (gray vectors) and from April to June (red vectors). The locations of the different estuarine water stations studied here are also shown. (For interpretation of the references to colour in this figure legend, the reader is referred to the web version of this article.)

River and the Northwest Atlantic Ocean (Fig. 1A). Circulation in the EGSL is therefore estuarine, with a lower-salinity surface layer flowing seawards and saltier subsurface and bottom layers flowing landwards (Koutitonsky and Bugden, 1991): (1) the thin, seaward-flowing surface layer (down to 50 m) has a temperature of 2–10 °C and a salinity of 25–32, and it originates from the mixing of seawater with freshwater runoff from the Great Lakes, the St. Lawrence River, and the northern Quebec drainage system; (2) a cold (−1 to 2 °C) and saline (31.5–33) subsurface layer (50–150 m) forms from the winter cooling of dense surface waters as tributary flow decreases and ice forms; and (3) a warmer (3–6 °C) and saltier (34–35) landward-flowing bottom layer (> 150 m deep) that originates from the edge of the continental shelf through mixing between cold, fresh, and oxygen-rich waters from the outer LCW and warm, salty, and oxygen-poor North Atlantic Central Water (NACW). In this bottom layer, the mixing proportion between the outer LCW and the NACW varies on a decadal or secular time scale

(e.g., Bugden, 1991; Gilbert et al., 2005, 2007; Thibodeau et al., 2010). Indeed, Gilbert et al. (2005) suggested a change in the relative proportion of outer LCW and NACW in the water mass entering the Laurentian Channel from the 1930s to the 1980s. Based on instrument temperature and salinity measurements of the outer LCW and the NACW, these authors propose that the Laurentian Channel bottom waters were composed of approximately 72% LCW and 28% NACW in the 1930s and approximately 53% LCW and 47% NACW in the 1980s.

The annual mean circulation in the EGSL is principally characterized by coastal currents with dominantly E–W flow, such as the Gaspé Current, the Anticosti Gyre, and the inflowing West Newfoundland Current, which flows northward along the west coast of Newfoundland (Fig. 1B). These currents are characterized by a mean speed on the order of ~1 cm/s (Tang, 1980). In the EGSL, one of the most striking features of near-surface circulation is the Gaspé Current, which is a buoyancy-driven coastal jet that originates in the St. Lawrence Estuary (near Rimouski), flows seaward along the coast of the Gaspé Peninsula (Sheng, 2001) and finally exits the gulf through the Cabot Strait. The tidal pulse from the Atlantic Ocean enters the Gulf of St. Lawrence from two directions, through the Cabot Strait and Strait of Belle Isle (Fig. 1B). Water mass circulation through the Strait of Belle Isle is mainly characterized by a branch of the inner LCW that flows southwest along the Labrador coast into the Gulf of St. Lawrence (Fig. 1B). The Cabot Strait represents a direct connection between the EGSL and the Northwest Atlantic Ocean, where seawater masses passing through it are characterized by a mixture of the NACW and the outer LCW (Gilbert et al., 2005). Notably, in addition to tidal pulses from the Atlantic Ocean, internal tides and waves can also be responsible for sediment remobilization in the EGSL (e.g., Normandeau et al., 2014).

2.3. Sediment and seawater εNd and $^{87}Sr/^{86}Sr$ variations in eastern Canada and adjacent continental shelves

The lithogenic Nd isotopic signature of sediments from the eastern Canadian Shield shows that the glaciomarine sediments from the western basin of the Hudson Strait and Baffin Bay have very unradiogenic Nd isotope compositions (i.e., low $^{143}Nd/^{144}Nd$ ratios and εNd values) with εNd values ranging from −28 to −29 and −23 to −27, respectively (Piepgras and Wasserburg, 1987; Farmer et al., 2003; Rashid et al., 2012). The Precambrian crust of the North American Shield is also characterized by a very unradiogenic εNd signature (εNd ≈ −36 to −45; Innocent et al., 1997; Rashid et al., 2012; Hollings et al., 2008). Sediments originating from the Grenville Province have an unradiogenic Nd isotope composition (εNd ≈ −22; Farmer et al., 2003; Pratte et al., 2017; Fig. 1A) and a large range of $^{87}Sr/^{86}Sr$ signatures of 0.70982–0.77457 (Millot et al., 2002; Namur et al., 2010). The Appalachian Province in the southern part of the EGSL records a Panafrican Nd isotope signature (εNd ≈ −10 to −14; Hollings et al., 2008; Fagel and Hillaire-Marcel, 2006a; Phan et al., 2018; Fig. 1A) and $^{87}Sr/^{86}Sr$ values of 0.71110–0.76329 (Portier, 2015; Vinciguerra et al., 2016; Phan et al., 2018). Overall, as εNd and $^{87}Sr/^{86}Sr$ vary widely according to the different geological provinces present in eastern Canada, we can use sediment εNd and $^{87}Sr/^{86}Sr$ signatures to reconstruct sediment provenance changes in the EGSL (e.g., Farmer et al., 2003).

In the eastern part of the Strait of Belle Isle and north of Newfoundland, the modern inner LCW has unradiogenic εNd values ranging from −26 to −23 (Piepgras and Wasserburg, 1987; Filippova et al., 2017), clearly documenting terrestrial inputs from the Precambrian terrains of the Canadian Shield (e.g., Farmer et al., 2003; Rashid et al., 2012). In contrast, the outer LCW is currently characterized by more radiogenic εNd compositions with mean values ranging between −15 and −14 around the tail of the Grand Banks of Newfoundland, likely reflecting mixing with water masses that have more radiogenic isotopic signatures, such as WGC, BC, the Irminger Current, and the North Atlantic Current (Lacan and Jeandel, 2004; Lacan et al., 2012; Filippova et al., 2017; Fig. 1A). Seawater from Baffin Bay exhibits very unradiogenic εNd values (−25), dominated by Archean sources (Stordal and Wasserburg, 1986). Conversely, the NACW (which originates in the temperate Northwest Atlantic) is characterized by the most radiogenic εNd values in the area, ranging from −11 to −9 (Tachikawa et al., 1999; Lacan et al., 2012; Lambelet et al., 2016; Fig. 1A).

3. Materials and methods

A total of 12 core-top sediment samples were collected at different depths in the EGSL and adjacent continental shelves (Fig. 1; Table S1) during several oceanographic missions on board the R/V Coriolis II (COR-05, −06, −09 and −10), the Marion Dufresne (MD-99) and the Canadian Coast Guard Ship Hudson (HU-2003). The sampling of the uppermost 1 cm of sediment (core-top) was performed using a box core, trigger weight core and/or piston core sampler (Table S1). The box core (BC) sampler is designed for recovering a relatively undisturbed sample of the sediment-water interface. Likewise, the trigger weight corer (TWC) collected in conjunction with a piston corer (PC) also allows recovery of the sediment-water interface, which is usually perturbed when the piston corer enters the sediments. Thus, the core-top (0–1 cm) sediments sampled with the BC and TWC are assumed to have recovered the sediment-water interface, while this may not necessarily be the case with the PC. Only core MD99–2236 was sampled with a long Calypso piston core system. Based on the fact that the modern sedimentation rates in the EGSL diminish exponentially from approximately 0.74 cm/yr at the head of the estuary to 0.15–0.20 cm/yr in the gulf to approximately 0.01 cm/yr at the mouth of the Laurentian Channel in the Atlantic (e.g., Smith and Schafer, 1999; Muzuka and Hillaire-Marcel, 1999; St-Onge et al., 2003; Barletta et al., 2010; Genovesi et al., 2011; Thibodeau et al., 2013), we can therefore estimate the these core-top sediment samples represent, on average, modern times or at least younger than the last 170 years, except for core MD99-2236, in which the core-top represents around 425 years according to Jennings et al. (2015). To compare the Nd isotopic data derived from the Fe—Mn oxyhydroxide coatings of sediment particles, 15 water samples from three different depths were recovered from 5 stations (COR1206-030, COR1206-025, COR1207-003, COR1207-007, and COR1503-007, hereinafter referred to as S1, S2, S3, S4, and S5, respectively) along the axis of the Laurentian Channel, from its head to its mouth, during the cruises COR1206, COR1207, and COR1503 of the R/V Coriolis II in the fall of 2012 and the summer of 2015 (Fig. 1B; Table S2). Estuarine water samples were collected with a rosette equipped with 12 Niskin-type sample bottles and several Seabird sensors (conductivity, temperature, pressure, and beam transmission). The bottom water samples were collected in the benthic nepheloid layer (~10 m above the seafloor). The water samples were transferred into 20-L acid-cleaned LDPE collapsible cubitainers and stored in a cold room. All water samples were filtered in the laboratory using a 0.45 µm membrane (Millipore Corp.) and then acidified to a pH of ~2 with Suprapur 6 M HCl, following GEOTRACES recommendations (van de Flierdt et al., 2012).

Detailed descriptions of the methods are provided in the supplementary material. Briefly, the preconcentration of REEs of estuarine water was performed following the analytical procedures outlined in Shabani et al. (1992) and Jeandel et al. (1998). Nd and Sr isotope compositions from the authigenic Fe—Mn coatings of bulk sediment were extracted following the leaching protocol of Chen et al. (2012). The residual fraction remaining after leaching the bulk sediment (i.e., the detrital fraction) was digested using a hydrofluoric-nitric-perchloric ($HF\text{-}HNO_3\text{-}HClO_4$) procedure modified from Révillon and Hureau-Mazaudier (2009). Sr and Nd were separated from other elements using a single-step ion chromatographic separation process (Li et al., 2014). Subsequently, REE concentrations were determined using an inductively coupled plasma quadrupole mass spectrometer (ICP-QMS Agilent 7500c) at the *Institut des sciences de la mer de Rimouski* (ISMER, Canada). Sr isotope ratios ($^{88}Sr/^{86}Sr$) were measured in dynamic mode on a Thermo Scientific Triton Plus™ multicollector thermal ionization

mass spectrometer (TIMS) at GEOTOP (Montreal, Canada). Finally, Nd isotope ratios ($^{143}Nd/^{144}Nd$) were analyzed on a Nu Instruments multicollector inductively coupled plasma mass spectrometer (MC-ICP-MS), also at GEOTOP.

The REE measurements were normalized to the Post-Archaean Australian Shale (PAAS, Pourmand et al., 2012). Hence, the subscript "n" indicates PAAS-normalized abundances. Based on several geochemical studies that addressed REE concentrations in authigenic phases and seawater (Haley et al., 2004; Molina-Kescher et al., 2014; Osborne et al., 2015; Laukert et al., 2017), we used the HREE/LREE ratio (Yb_n/Nd_n) to investigate the fractionation between HREEs and LREEs. Similar to the processes used in other sediment provenance studies (e.g., Armstrong-Altrin et al., 2013, 2016), in the detrital fraction, HREE versus LREE enrichment was quantified by (La/Yb)n, HREE versus MREE enrichment was quantified by (Gd/Yb)n, and the Eu anomaly was quantified as follows: $Eu/Eu^* = Eu_n/(Sm_n*Gd_n)^{1/2}$. Nd isotope ratios are expressed as follows: $\varepsilon Nd = ([(^{143}Nd/^{144}Nd)_{sample}/(^{143}Nd/^{144}Nd)_{CHUR}]-1)x10000$ (CHUR: chondritic uniform reservoir; Jacobsen and Wasserburg, 1980).

4. Results

4.1. Seawater physical properties

The potential temperature (θ), salinity, and potential density (σ_θ) of water masses from the five estuarine stations (S1, S2, S3, S4, and S5) studied here show similar hydrographic properties (Fig. 2A). In the surface layer, the five stations have a low salinity (28.2–31.5), a high temperature (3–9 °C), and a low potential density (21.9–25.5 kg/m^3). The subsurface layer has salinity values of 31.5–33.0, cold temperatures of −1.0–2.5 °C, and potential density values of 25.5–26.5 kg/m^3. The bottom layer exhibits the highest salinity (34–35), a high temperature (4.0–6.7 °C), and a high potential density (27–28 kg/m^3).

In general, surface and bottom layers have lower beam transmission intensities (82–92%) than the subsurface layer (97–100%) (Fig. 2B). Based on these data, nepheloid layers were identified between 250 and 310 m in the lower St. Lawrence Estuary and between 420 and 500 m at station S5 in the gulf (Fig. 2B).

4.2. REE concentrations

The PAAS-normalized REE fractionation patterns are shown in Figs. 3 and 4. The Nd concentrations from the detrital and bulk sediment leachates samples ranged from 16 to 34 μg/g and from 0.05 to 1.4 μg/g, respectively (Tables S4 and S5). The PAAS-normalized REE patterns of the detrital sediment samples display patterns with moderate LREE enrichment, slightly depleted to flat HREEs and significant positive Eu anomalies (Eu/Eu* > 1.3; Table S4; Fig. 3A). These LREE-enriched patterns were also evidenced by high (La/Yb)n and (Gd/Yb)n ratios (Fig. 5C; Table S4). However, note that the sediments from the Labrador Shelf (MD9922–36) have the highest LREE and MREE enrichment. Likewise, sediments from the Laurentian and Esquiman channels have higher (La/Yb)n and (Gd/Yb)n ratios than sediments from the shelf (Fig. 5C). Moreover, the PAAS-normalized REE patterns of the bulk sediment leachates from the EGSL reveal an MREE bulge-type pattern (Fig. 3B), with greater enrichment of MREEs than of HREEs and LREEs, which is a common pattern in leachates and authigenic material supplied by rivers (Haley et al., 2004; Gutjahr et al., 2007; Du et al., 2016; Abbott et al., 2016).

The PAAS-normalized REE patterns in most water samples from the EGSL display patterns characterized by a pronounced negative Ce anomaly together with HREE enrichment (Fig. 4). The negative Ce anomaly is generally more pronounced in the most saline deeper water samples than in the surface and subsurface samples or in the gulf samples. However, some surface and subsurface water samples from stations S1 to S4 have relatively flat REE patterns with little to no Ce anomaly. The dissolved LREE concentrations (represented in this study by Nd) from all of the water stations in the EGSL show a decreasing trend with depth, i.e., from 22 pmol/kg in the surface and subsurface waters to 2.5 pmol/kg in the most saline bottom water samples (Fig. 6A and 7A; Table S6). This decreasing trend in the LREE concentrations is exactly opposite to the pattern observed in the open ocean, in which the surface features lower concentrations than the bottom (e.g., Zhang and Nozaki, 1996). The range of Nd concentrations in the analyzed water samples is comparable with previously published values from estuarine and coastal waters with a similar salinity range (28 to 35) and strong riverine influence (3 to 60 pmol/kg; Sholkovitz and Szymczak, 2000,

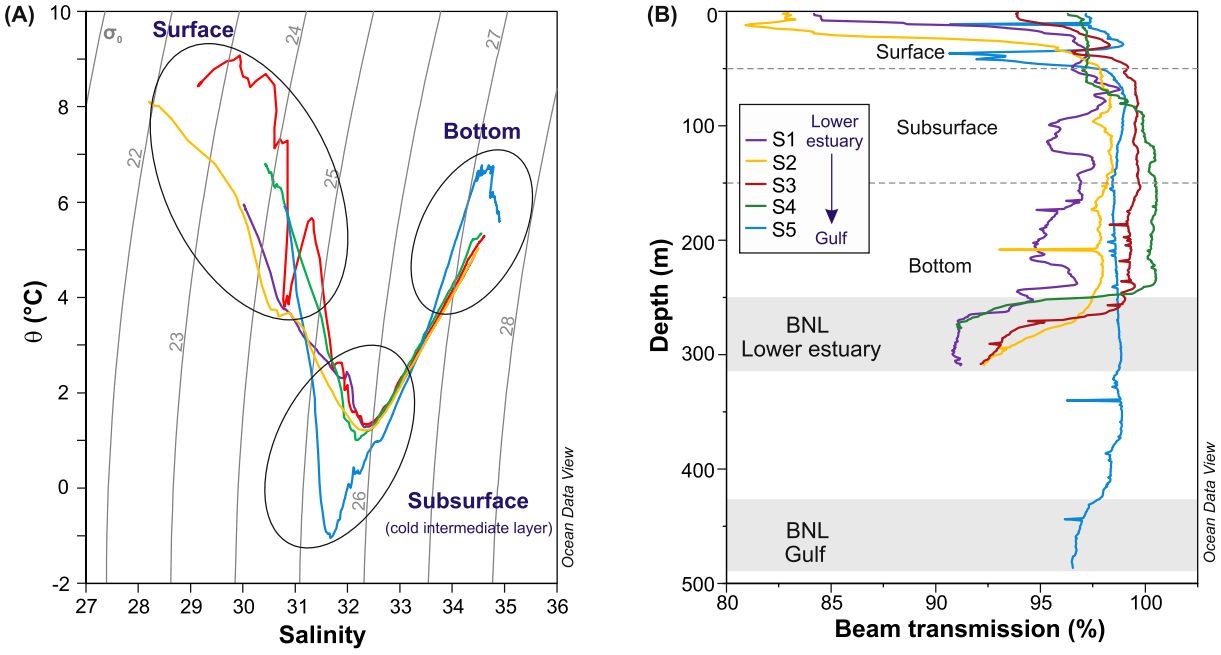

Fig. 2. (A) Potential temperature (°C) versus salinity plot with potential density isopycnals (solid gray lines; σ_θ = potential density at reference pressure 0 m) for the five seawater stations analyzed in this study. Three distinctive sea water layers can be distinguished: a surface layer, a cold and saline subsurface layer, and a warmer and saltier bottom layer. This diagram was constructed using the ODV software (Schlitzer, 2017). (B) Vertical distribution of beam transmission data (% light attenuation) measured at the five estuarine water stations in the EGSL. BNL: benthic nepheloid layer.

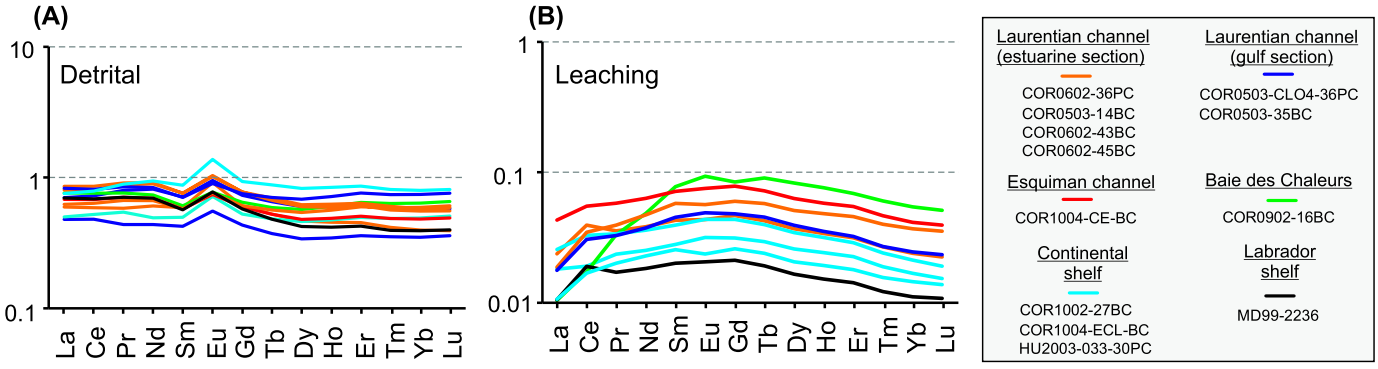

Fig. 3. (A) REE patterns normalized to PAAS for the detrital sediment samples. (B) REE patterns normalized to PAAS for the leachate sediment samples.

Osborne et al., 2014; van de Flierdt et al., 2016). Likewise, most of the dissolved $(HREE/LREE)_n$ profiles in the EGSL (except station S3) show a decrease in the first 50 m and then an increasing trend with depth (Fig. 6B). The dissolved $(HREE/LREE)_n$ ratios of surface water samples also show an increasing trend from the estuary to the gulf stations.

4.3. Sr and Nd isotope signatures

The Sr and Nd isotope data obtained from the detrital sediments, bulk sediment leachates and estuarine water are provided in Table S7. The detrital sediment samples feature $^{87}Sr/^{86}Sr$ values ranging between 0.71475 and 0.73062 (median 0.72351), which are higher than the values of the other sample types here studied. Indeed, the $^{87}Sr/^{86}Sr$ values obtained from the bulk sediment leachates and estuarine water samples range between 0.70975 and 0.70870 (median 0.70925) and between 0.70915 and 0.70937 (median 0.70921), respectively (Fig. 5A). These values are close to the modern values from the shelf and oceanic waters (0.70917 ± 0.00002; El Meknassi et al., 2018).

The εNd values obtained from the detrital sediment samples (Figs. 5A-B and 8A; Table S7) range between −14.3 (Baie des Chaleurs) and − 28.7 (southern Labrador Shelf). The detrital εNd values from the estuary range between −18.7 and − 21.8, whereas the detrital εNd values from the mouth and the continental shelves are more radiogenic, with values ranging from −14.3 to −16.

Replicate εNd analyses of two bulk sediment leachate samples (COR0602-36PC and COR0503-CL04-36PC) yielded similar εNd values within analytical uncertainty (Table S7). This similarity indicates a robust level of reproducibility for the entire analytical procedure used in our study. Such reproducibility of εNd analyses in bulk sediment leachates indicates that variations of approximately 2 ε units could be considered significant. The εNd values of bulk sediment leachates from the EGSL range between −16.1 (Baie des Chaleurs) and − 27.2 (southern Labrador Shelf) (Figs. 5A-B and 8B-C; Table S7). Bulk sediment leachate samples from the lower estuary have more unradiogenic εNd values (approximately −20), whereas samples from the mouth and continental shelves have slightly more radiogenic εNd values (approximately −18). Furthermore, the εNd values from the bulk sediment leachates and the detrital fraction display a significant positive linear correlation ($r = 0.88$; $n = 10$; Fig. 8C).

The εNd values obtained for the estuarine water mass range between −19 and − 22 (Figs. 5A, 6C and 9; Table S6). No significant differences in εNd values between the surface waters and the most saline bottom waters from the same stations are observed (Figs. 6C, 7B, and 9). The most radiogenic εNd values are observed at stations closest to the South Shore (S2 and S4; εNd = −17 to −18), and the least radiogenic Nd isotope compositions are observed at stations closest to the North Shore and the gulf (S1, S3, and S5; εNd = −19 to −22).

5. Discussion

To assess the influence of the input of lithogenic riverine material on the estuarine water chemistry of the EGSL, we first discuss the detrital REE and Nd−Sr isotope patterns and their implications for identifying different source areas and transport pathways of detrital material in eastern Canada. We then compare the authigenic REE concentrations and Nd−Sr isotope values extracted from the bulk sediment leachates with the values in the overlying water column and in the detrital fraction to identify the main phase extracted during the leaching process. Furthermore, we evaluate the potential influence of estuarine processes and terrestrial inputs on the REE distribution and εNd signals of the estuarine waters in the EGSL.

5.1. Detrital REE and Nd−Sr isotope patterns in surface sediments in eastern Canada: tracing potential sediment sources

The PAAS-normalized REE patterns of detrital sediments can provide important clues about source-rock characteristics (e.g., Montero-Serrano et al., 2009; Armstrong-Altrin et al., 2013, 2016; Osborne et al., 2015). Indeed, the significant positive Eu anomalies ($Eu/Eu^* > 1.3$; Table S4) observed in our detrital fraction are characteristic of sediments derived mainly from felsic igneous/metamorphic sources (e.g., Bayon et al., 2015). The positive Eu anomaly is generally attributed to the tendency of

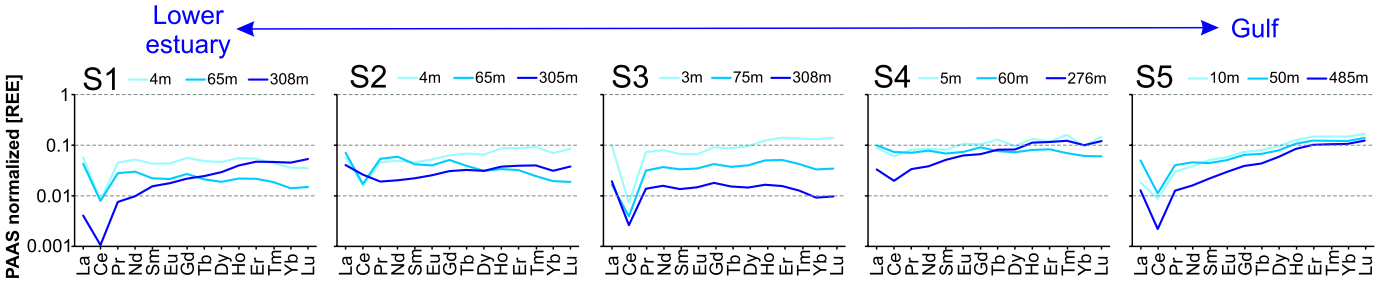

Fig. 4. REE patterns normalized to PAAS at different depths at the five estuarine water stations. The PAAS-normalized REE patterns in most water samples from the EGSL display a pronounced negative Ce anomaly and enrichment in the heavy REEs.

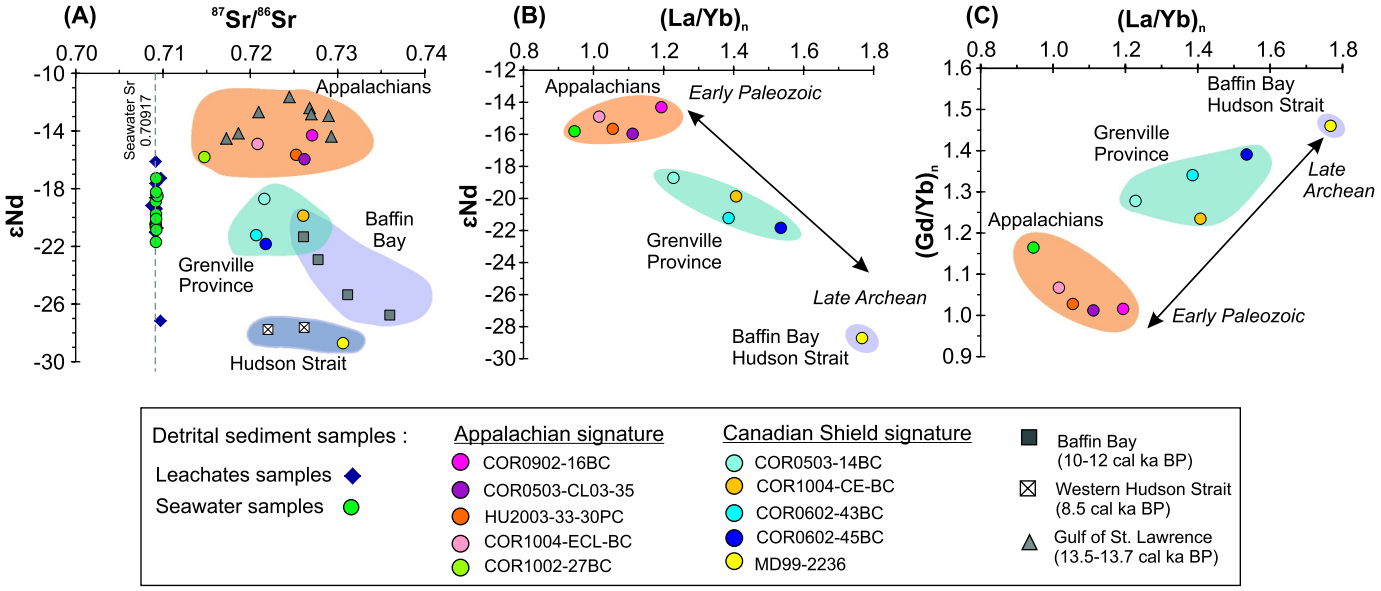

Fig. 5. Comparison of detrital sediment sample sources: (A) εNd versus $^{87}Sr/^{86}Sr$, (B) εNd versus (La/Yb)n, and (C) (La/Yb)n versus (Gd/Yb)n. The subscript "n" indicates PAAS-normalized abundances (Pourmand et al., 2012). Sediment samples from Baffin Bay, the western Hudson Strait, the southern Labrador Shelf, and the Gulf of St. Lawrence are also included (Fagel et al., 1999; Farmer et al., 2003). These three different detrital provinces are illustrated in colored arrays (gray, blue and orange). (For interpretation of the references to colour in this figure legend, the reader is referred to the web version of this article.)

europium to be preferentially incorporated into plagioclase (Weill and Drake, 1973). Several sedimentological and mineralogical studies (Loring and Nota, 1973; Jaegle, 2015; Casse et al., 2017) have suggested that modern sedimentary inputs in the EGSL are derived mainly from the Canadian Shield on the North Shore and are characterized by high proportions of plagioclase feldspar (32–65%), potassium feldspar (7–21%), and amphibole (1–7%) (Jaegle, 2015). Thus, the high input of plagioclase from the Canadian Shield to the EGSL could explain the positive Eu anomaly observed in the detrital fraction.

Furthermore, the $^{87}Sr/^{86}Sr$ values of detrital sediments from the EGSL are relatively radiogenic and range between 0.71475 and 0.73062 (Fig. 5A). These values are consistent with the $^{87}Sr/^{86}Sr$ data from the Grenville Province (0.70982 to 0.77457; Millot et al., 2002; Namur et al., 2010) and the Appalachian Mountains (0.71110 to 0.76329; Portier, 2015; Vinciguerra et al., 2016; Phan et al., 2018). However, as the $^{87}Sr/^{86}Sr$ values from the Grenville and Appalachian domains overlap, it is difficult to distinguish between these sources of sediment in the EGSL based only on Sr isotopes. Therefore, we combine (La/Yb)n and (Gd/Yb)n ratios with Sr and Nd isotopes to better track the origin of the sediment (Fig. 5). The diagrams reveal two distinctive sedimentary sources: the Appalachian domain and the Canadian Shield (including the Grenville, Nain, and Makkovik provinces; Fig. 1).

The surface sediment samples collected on the Canadian continental shelf (COR1002-27BC, COR1004-ECL-BC, 2003-033-30PC, and COR0503-CL03-35BC) and at Baie des Chaleurs (COR0902-16BC) have εNd values ranging between −14.3 and − 16.0, high $^{87}Sr/^{86}Sr$ ratios ranging between 0.71475 and 0.72708, low (La/Yb)n values ranging from 0.95 to 1.19, and low (Gd/Yb)n values of 1.02 to 1.16 (Fig. 5). Taking into consideration the εNd values of the Grenville Province (εNd ≈ −22; Farmer et al., 2003; Pratte et al., 2017) and the Appalachian Province (εNd ≈ −11; Fagel and Hilaire Marcel, 2006; Phan et al., 2018) and using a conservative binary mixing, we estimated that the Nd isotope composition of these samples is 61% from Appalachian sources and only 39% from the Grenville Province (Fig. 10). Farmer et al. (2003) identified a similar range of εNd values in deglacial sediments from the Gulf of St. Lawrence. Based on coastal current

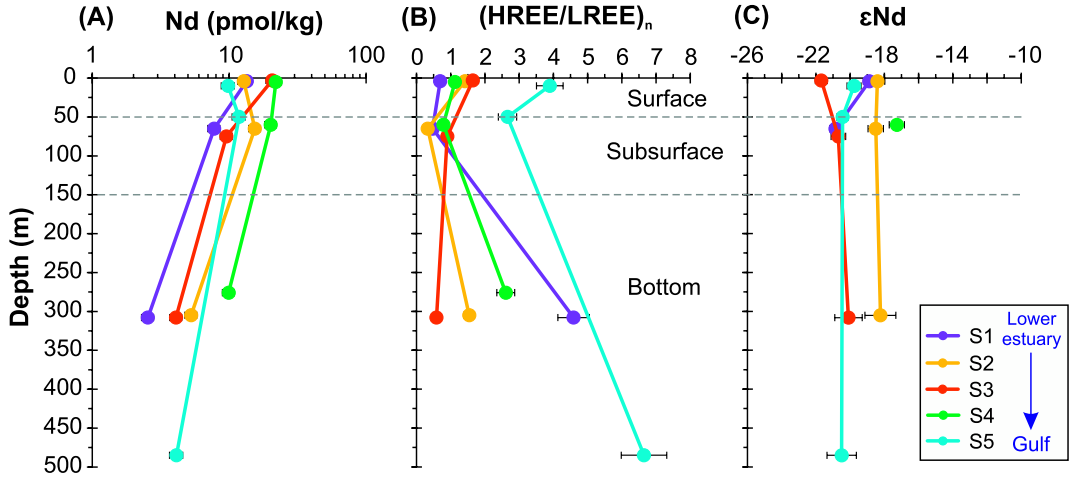

Fig. 6. Vertical distribution of (A) Nd concentrations, (B) PAAS-normalized HREE/LREE ratios, and (C) εNd values obtained from the five estuarine water stations. For a better illustration of the data distribution, a logarithmic scale for Nd concentrations is used. Error bars represent the external 2-sigma errors.

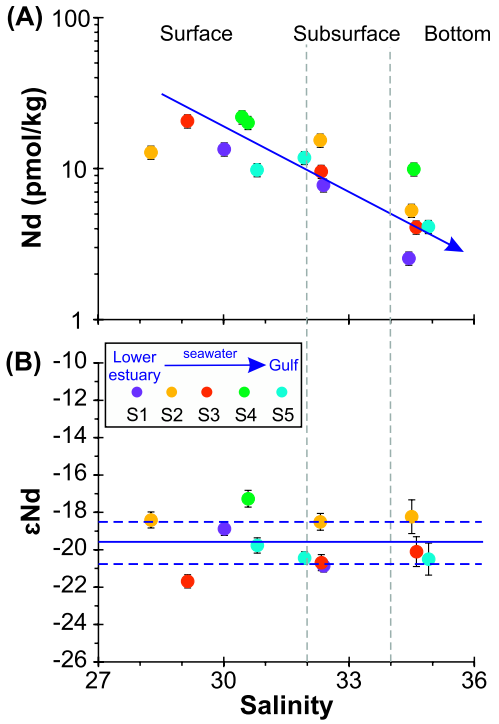

Fig. 7. Scatter plots of salinity versus (A) Nd concentration and (B) εNd values for the five estuarine water stations. For a better illustration of the data distribution, a logarithmic scale for Nd concentrations is used. In (B), the blue lines represent the mean (bold line; −19.6) and the standard deviation (dashed line; ±1.2) of all of the εNd data. The salinity versus Nd concentration plot shows a decreasing trend, while the salinity versus εNd plot does not exhibit significant differences between the surface waters and the most saline bottom waters from the same stations. (For interpretation of the references to colour in this figure legend, the reader is referred to the web version of this article.)

patterns in the EGSL (Galbraith et al., 2016), we suggest that the Appalachian sediments observed in these surface sediment samples are mainly transported via the Gaspé Current (Fig. 1B). This coastal current separates into two branches downstream of the tip of the Gaspé Peninsula; the southern branch flows over the Magdalen Shelf and along the coast of the Canadian Maritime Provinces, whereas the northern branch flows along the western edge of the Laurentian Channel (Trites, 1972; Sheng, 2001). Thus, the southern branch forms the main outflow of the gulf on the western side of Cabot Strait and may therefore transport Appalachian sediments from the South Shore and Canadian Maritime Provinces to the gulf and then to the continental shelf off southeastern Canada through the Cabot Strait (Loring and Nota, 1973; Dufour and Ouellet, 2007; Casse et al., 2017).

The sediment samples from the Laurentian (COR0503-CL04-36PC, COR0503-14BC, COR0602-043BC, COR0602-045BC, COR0602-36PC) and Esquiman (COR1004-CE-BC) channels feature low εNd values (−18.7 to −21.8), high $^{87}Sr/^{86}Sr$ values (0.72068 to 0.72607), and relatively high (La/Yb)n and (Gd/Yb)n values (1.23 to 1.53 and from 1.28 to 1.39, respectively; Fig. 5), which are characteristic of the Canadian Shield source rocks (Farmer et al., 2003; Pratte et al., 2017). The overall Nd signature of the Canadian Shield is difficult to assess because these terranes are very complex and vary greatly in age (1.8–3.8 Ga; Innocent et al., 1997). The Nd isotope ratios from terranes belonging to the Canadian Shield record unradiogenic εNd values of −35.9 to −22 (Revel et al., 1996; Innocent et al., 1997; Dickin, 2000; Rashid et al., 2012; Pratte et al., 2017). According to Fig. 10, detrital sediments from the Laurentian and Esquiman channels are characterized by a mixed detrital source; in other words, they are mainly from the Grenville Province (86%) but feature a notable contribution from the Appalachian Mountains (14%). The sediment samples from the Esquiman

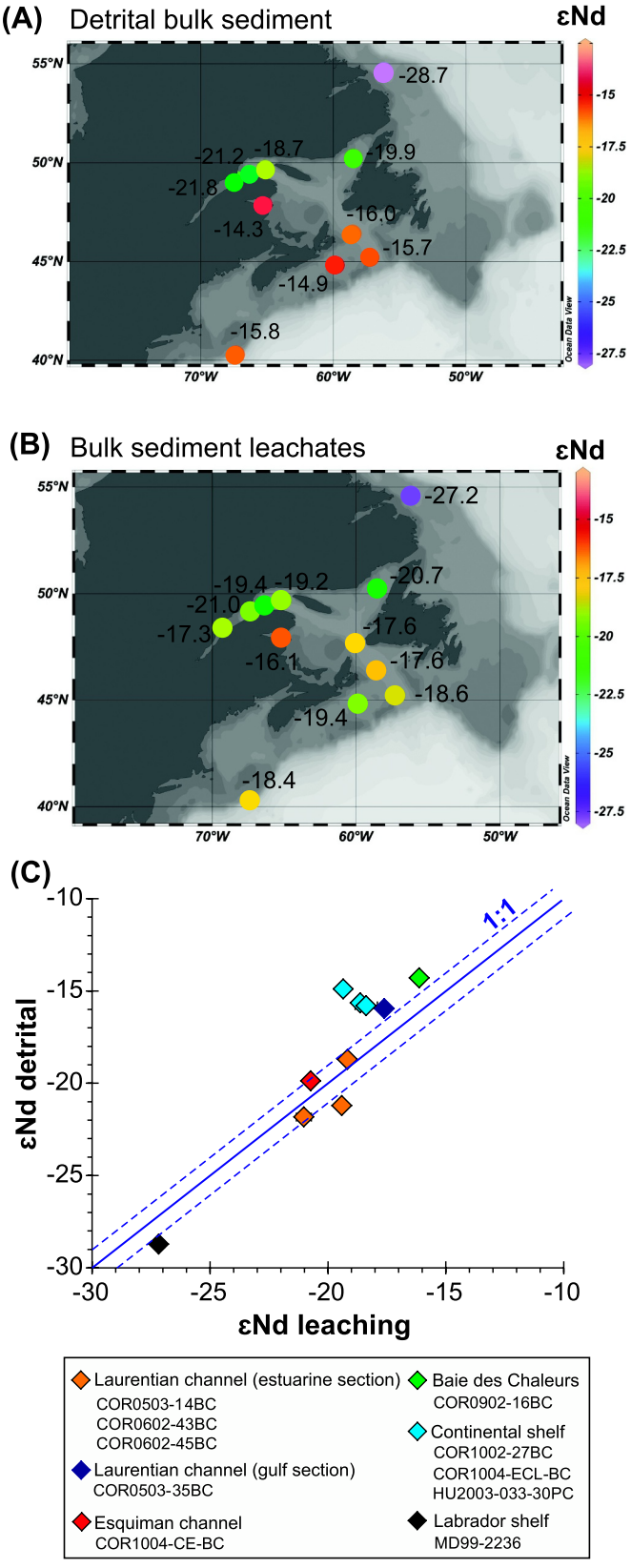

Fig. 8. Spatial distribution of εNd values obtained from the (A) detrital surface sediments and (B) bulk sediment leachates. (C) εNd values of bulk sediment leachates versus those of detrital sediments. The external 2-sigma errors are represented by the symbol size. The blue line corresponds to the 1:1 slope. Larger differences between those two fractions (ΔεNd > 3) are likely due to sample heterogeneity combined with unwanted chemical extraction of other phases during sequential leaching.(For interpretation of the references to colour in this figure legend, the reader is referred to the web version of this article.)

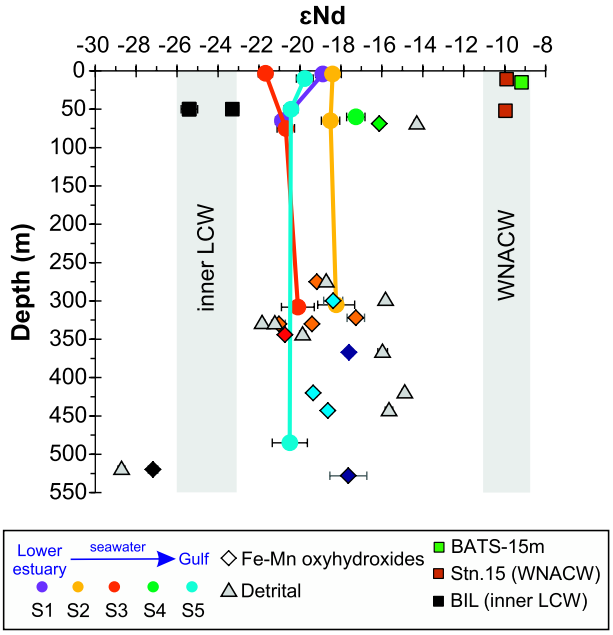

Fig. 9. Vertical profiles of εNd values obtained from estuarine waters, bulk sediment leachates, and detrital sediments are shown. Seawater samples from the inner LCW (station BIL; Filippova et al., 2017) and the Western North Atlantic Central Water (WNACW; typified by the Bermuda Atlantic Time Series Station BATS-15m and Stn. 15; van de Flierdt et al., 2012; Lambelet et al., 2016) are also included. The Nd isotopic compositions of the bulk sediment leachates and estuarine waters in the EGSL mainly reflect the unradiogenic εNd signature of the Canadian Shield (εNd ≈ −22 to −18). Error bars represent the external 2-sigma errors.

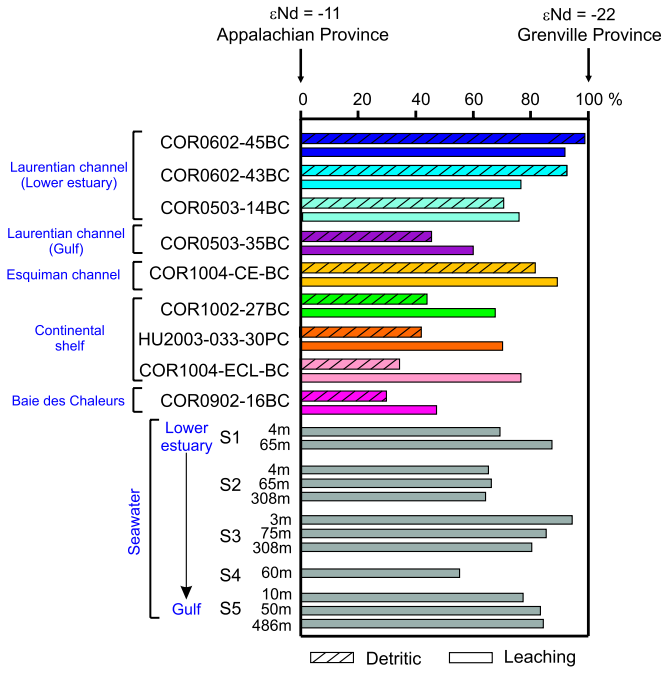

Fig. 10. Relative contribution of the Appalachian source vs. the North American Shield. The relative percentages were calculated with the Nd isotope composition from the North American Shield ($^{143}Nd/^{144}Nd$ = 0.51105; Innocent et al., 1997) and Appalachian sources ($^{143}Nd/^{144}Nd$ = 0.512045; Fagel and Hilaire Marcel, 2006a) according to $^{143}Nd/^{144}Nd_{(\%Grenville\text{-}Prov)}$ = [[($^{143}Nd/^{144}Nd_{sample}$) – (0.512045-0.51105)]/ (0.512045-0.51105)]*100.

Channel have higher $^{87}Sr/^{86}Sr$ values (up to 0.72607) than the sediment from the Laurentian Channel (Fig. 5A), probably due to their proximity to the Strait of Belle Isle, which is influenced by the inner LCW (Petrie and Anderson, 1983). Because the inner LCW transport large amounts of dissolved and suspended particulate material with distinctive geochemical signatures from the Hudson Strait and the Labrador continental margin (Lacan and Jeandel, 2005), this current can influence the geochemical composition of the surface sediments in the Esquiman Channel. However, further investigations are needed to gain a more precise understanding of the sediment contributions from the Hudson Strait and Labrador continental margin to the Esquiman Channel.

Finally, the sediment sample from the southern Labrador Shelf (Cartwright Saddle; MD99–2236) has an εNd value of −28.7, a $^{87}Sr/^{86}Sr$ value of 0.73062, a high (La/Yb)n value (approximately 1.77), and a high (Gd/Yb)n value (approximately 1.46) (Fig. 5). These Nd and Sr isotope values are characteristic of the Hudson Strait and Baffin Bay sediments (Farmer et al., 2003), which are characterized by unradiogenic εNd values (~ −28.1 to −28.9 and − 23.1 to −27.2, respectively) and high $^{87}Sr/^{86}Sr$ values (0.72205 to 0.72619 and 0.72611 to 0.73600, respectively). These unradiogenic εNd values may be associated with increased detrital Nd and Sr inputs to this area by the inner LCW, which ultimately delivers Nd and Sr eroded from the eastern Canadian Shield (Farmer et al., 2003; Lambelet et al., 2016; Filippova et al., 2017).

5.2. *REE and Sr isotope values of bulk sediment leachates: Fingerprint of the authigenic Fe–Mn oxyhydroxide fraction*

The REE distributions and $^{87}Sr/^{86}Sr$ values obtained from bulk sediment leachates can be used to demonstrate the absence of detrital contamination during the leaching process and, thus, to indicate that the REE and Nd isotope signals extracted from bulk sediment samples are derived entirely from seawater (e.g., Gutjahr et al., 2007; Molina-Kescher et al., 2014; Du et al., 2016). The PAAS-normalized REE plot of the bulk sediment leachate data shows significant MREE enrichment (Fig. 3B), which is not present in the detrital sediment samples (Fig. 3A). This MREE-enriched pattern is typical of Fe–Mn oxyhydroxide and riverine particulate leachates (e.g., Haley et al., 2004; Gutjahr et al., 2007; Du et al., 2016; Abbott et al., 2016), suggesting that these phases were principally extracted from the bulk sediment samples. Moreover, as local rivers in the EGSL clearly play a predominant role in the input of REEs (Gaillardet et al., 2003), we hypothesize that the REE patterns leached from bulk sediment samples likely represent a mixture of locally formed and pre-formed continental Fe–Mn oxyhydroxides (e.g., Bayon et al., 2004; Poulton and Raiswell, 2005; Kraft et al., 2013). Alternatively, the MREE enrichment observed in our bulk sediment leachates could also be caused by the dissolution of phosphates, such as apatite (Hannigan and Sholkovitz, 2001; Pourret and Tuduri, 2017). With the data currently available, we cannot validate or reject this last hypothesis. However, apatite appears to be negligible in the sediment samples from the main rivers that feed the EGSL (Jaegle, 2015) and marine sediments from the Laurentian Channel (Casse et al., 2017), as suggested by its low abundance (<0.1%) or absence in the quantitative phase analysis (X-ray powder diffraction method developed by Eberl, 2003 and Eberl and Smith, 2009) of X-ray diffractograms of bulk sediment samples (Fig. S1). Likewise, the remineralization of organic compounds in estuarine and coastal marine sediments could also explain (at least partly) the REE distribution in the bulk sediment leachates (Bayon et al., 2004; Freslon et al., 2014). However, even if organic matter dominated the MREE bulge-type pattern, the dissolution of organic compounds during the leaching processes would lead to an REE pattern 10 times more enriched than the PAAS abundances (e.g., Freslon et al., 2014). Because our sediment leachates are not characterized by a similar REE enrichment, we propose that the sedimentary organic matter fraction was not

extracted in our bulk sediment leachates.

Further evidence of the authigenic origin of the REEs in the bulk sediment leachates can be obtained from $^{87}Sr/^{86}Sr$ values (e.g., Haley and Polyak, 2013). The $^{87}Sr/^{86}Sr$ values obtained from the modern estuarine water samples and leachate sediment in the EGSL (median of 0.70921) are close to the global seawater value (Fig. 5A). The 2.4 Myr residence time of Sr in seawater is far longer than the mixing time of the oceans (1500 years; Broecker and Peng, 1982), causing a globally uniform $^{87}Sr/^{86}Sr$ value in seawater and modern marine carbonates ($^{87}Sr/^{86}Sr \approx 0.70917$; El Meknassi et al., 2018). This observation is especially relevant in the EGSL, where biogenic sources of carbonates are negligible (<1%; Jaegle, 2015; Casse et al., 2017) and detrital sediments typically have higher $^{87}Sr/^{86}Sr$ values (0.70982 to 0.77457; Millot et al., 2002; Namur et al., 2010; Vinciguerra et al., 2016; Phan et al., 2018).

Overall, all of these results suggest that authigenic Fe–Mn oxyhydroxide coatings are the dominant phase extracted in our bulk sediment leachates and that detrital and sedimentary organic matter contamination during the leaching procedure is negligible.

5.3. Dissolved REE and Nd isotope signatures of estuarine waters from the EGSL: Estuarine processes and potential influence of lithogenic inputs

The REE patterns of most of our water samples show a typical PAAS-normalized seawater REE pattern, which is characterized by a pronounced negative Ce anomaly together with progressive enrichment of heavy REEs (Fig. 4). This pattern is consistent with coastal waters and oceanic REE trends (e.g., Piepgras and Jacobsen, 1992; Rousseau et al., 2015; Filippova et al., 2017; Pourret and Tuduri, 2017). The negative Ce anomaly is attributable to the higher particle reactivity of Ce due to its specific redox properties and its oxidative state (IV) compared to the other trivalent REEs (Elderfield et al., 1990; Sholkovitz, 1993, 1995). As previously reported for estuarine mixing zones (e.g., Elderfield et al., 1990; Sholkovitz, 1993, 1995; Sholkovitz and Szymczak, 2000; Rousseau et al., 2015; Merschel et al., 2017; Pourret and Tuduri, 2017; Adebayo et al., 2018), the higher particle reactivity of Ce becomes amplified during salt-induced coagulation of colloids in estuaries and thus is responsible for the increase in the negative Ce anomaly with increasing salinity. Based on these considerations, we suggest that the decreasing trend observed in most of the dissolved LREE profiles (represented here by Nd) from the EGSL with depth and increasing salinity (Figs. 6A and 7A) can be attributed to the coagulation of colloidal material (Sholkovitz, 1993, 1995; Sholkovitz and Szymczak, 2000). Similar interpretations of dissolved metal concentrations in the St. Lawrence Estuary have been reported by Yeats and Loring (1991). Furthermore, bottom waters in the EGSL are characterized by decreased beam transmission (Fig. 2B), which are typically associated with suspended particulates in benthic nepheloid layers (e.g., Wu et al., 2015; Crocket et al., 2018). Thus, the lower Nd concentrations (~2.5 pmol/kg) and high (HREE/LREE)n ratios (>1) recorded in the near-bottom waters at each station may be linked to enhanced scavenging within the bottom nepheloid layer, likely through continuous adsorption of dissolved REEs onto Fe–Mn oxyhydroxide phases and/or any other detrital and authigenic phases.

Some surface and subsurface estuarine water samples (notably, S1-4 m, S1-65 m, S2-4 m, S3-75 m, S4-5 m, S4-60 m; Fig. 4) have relatively flat REE patterns with little to no Ce anomaly, suggesting a major influence of local river inputs and, therefore, an enhanced release of river-borne particulate REEs (Pourret and Tuduri, 2017). In this context, we examined the (HREE/LREE)n ratios versus εNd values to document the potential influence of the lithogenic inputs on the estuarine water chemistry of the EGSL (e.g., Osborne et al., 2015; Laukert et al., 2017). In the (HREE/LREE)n - εNd crossplot (Fig. 11), the REE data from detrital sediments fall in the mixed detrital zone, close to the Grenville [$\varepsilon Nd \approx -19$ to -21 and (HREE/LREE)n ≈ 0.4 to 0.7] and Appalachian [$\varepsilon Nd \approx -12$ and (HREE/LREE)n ≈ 1.1] signatures (Pratte et al., 2017; Phan et al., 2018). On the other hand, REE data from seawater samples from the inner LCW (stations BIL; Filippova et al., 2017), Gulf Stream (Bermuda Atlantic Time Series Station, BATS; van de Flierdt et al., 2012) and North East Atlantic Deep Water (station HL08; Filippova et al., 2017) form a well-constrained linear trend, here referred to as the seawater array. In general, most of the surface and subsurface estuarine waters (excluding the samples S2-4 m, S2-305 m, S3-3 m and all S5 water samples) and bulk sediment leachate samples from the EGSL are close to their potential detrital sources. These estuarine water samples were collected from within the lower St. Lawrence Estuary (Fig. 1B), in which the surface waters are characterized by a high suspended particulate matter content (up to 2.2 mg/L; Yeats et al., 1979; Larouche and Boyer-Villemaire, 2010). In agreement with previous geochemical studies in estuarine mixing zones (Sholkovitz, 1993, 1995; Sholkovitz and Szymczak, 2000; Freslon et al., 2014; Rousseau et al., 2015; Osborne et al., 2015; Merschel et al., 2017; Adebayo et al., 2018), we hypothesize that the (HREE/LREE)n values close to 1 in the surface and subsurface estuarine waters from the lower St. Lawrence Estuary may be the result of high rates of partial dissolution and release of river-borne particulate REEs.

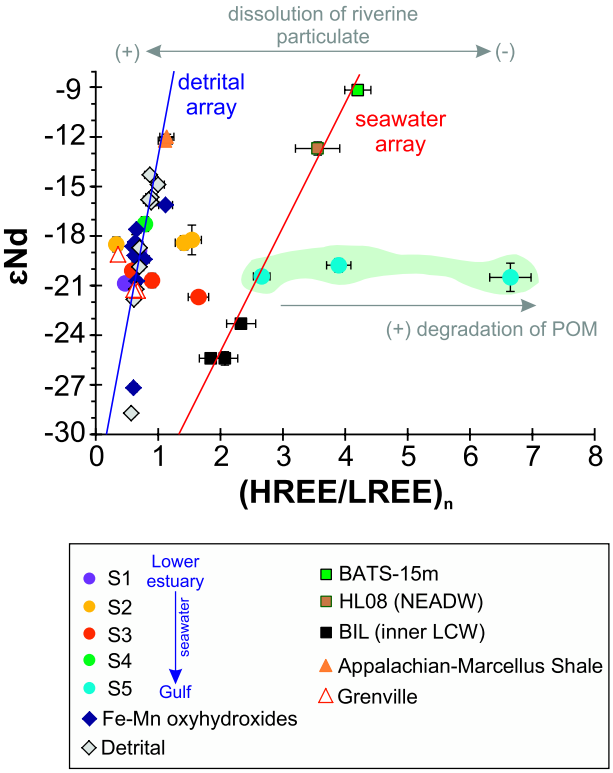

Fig. 11. (HREE/LREE)n - εNd crossplot including the detrital sediments, bulk sediment leachates and the estuarine waters analyzed in this study. Detrital sediments from the Grenville (Pratte et al., 2017) and Appalachian (Phan et al. 2018) provinces are shown. Seawater samples from the inner LCW (stations BIL; Filippova et al., 2017), the Western North Atlantic Central Water (Bermuda Atlantic Time Series Station BATS-15m; van de Flierdt et al., 2012) and the North East Atlantic Deep Water (NEADW; station HL08; Filippova et al., 2017) are also included.

The (HREE/LREE)n - εNd crossplot also suggests that additional estuarine processes involving the removal and addition of REEs may be of local importance in the EGSL. The closest seawater station to Cabot Strait (S5) exhibited the highest (HREE/LREE)n value (> 2) (Fig. 11). This zone is characterized by a low suspended particulate matter content in the surface waters (0.2 to 0.4 mg/L; Larouche and Boyer-Villemaire, 2010), reducing the potential for partial dissolution of riverine particulate material (Rousseau et al., 2015). In the gulf, these environmental conditions, in conjunction with increasing distance from

the detrital source and intense degradation of particulate organic matter in the water column (Mai-Thi et al., 2017), may be responsible for the continuous preferential removal of LREEs over HREEs from the dissolved load (e.g., Sholkovitz, 1993, 1995; Sholkovitz and Szymczak, 2000) and, therefore, for the increase in the (HREE/LREE)n ratio. In addition, the S2-4 m, S2-305 m, and S3-3 m water samples exhibited intermediate (HREE/LREE)n values (1.4 to 1.7). These stations are located in zones of important vertical mixing of water masses due to cyclonic structures, the Anticosti Gyre and the Gaspé Current (Dufour and Ouellet, 2007; Galbraith et al., 2016). Thus, the intermediate (HREE/LREE)n values recorded at stations S2 and S3 are probably the result of a combination of estuarine processes involving the partial dissolution of riverine detrital particles and remineralization of estuary sediments (e.g., Lawrence and Kamber, 2006).

On the other hand, the vertical distribution of dissolved εNd at all estuarine stations shows unradiogenic Nd isotope values throughout the entire water column (average εNd ~ −19.6 ± 1.2; Figs. 6C and 7B), and the values are similar to the εNd (±2σ) values of the detrital and bulk sediment leachate samples (Fig. 9). Because terrigenous suspended particles have a short residence time of a few days within the St. Lawrence Estuary (Syvitski et al., 1983; Lucotte et al., 1991) and the water depth in the EGSL is quite low (<500 m), we hypothesize that rapid scavenging by the salt-induced coagulation of colloidal matter and subsequent dissolution of the labile mineral phases influenced the εNd values in the water column of the EGSL. Moreover, the EGSL is considered to be a subarctic region, with air temperatures below zero degrees Celsius during the winter, allowing the formation of sea ice (Saucier, 2003; De Vernal et al., 2011). Diagrams of the winter temperature and salinity data from a station south of Anticosti Island (Galbraith, 2006) reveal that during winter, the upper 120 m of the water column is characterized by a high salinity (approximately 31.8) and near-freezing temperatures (approximately −2 °C) due to cooling and brine rejection during ice formation. Thus, brine rejection during sea ice formation may also play a significant role in the distribution of the relatively homogeneous Nd isotope values in EGSL seawater (Haley and Polyak, 2013). The flow from the surface to the bottom of the high-density brines may homogenize the Nd isotope composition of the water column. Similar observations have been reported by Porcelli et al. (2009), Haley and Polyak (2013) and Laukert et al. (2017) in the Arctic Ocean.

In summary, although we acknowledge that the low spatial and vertical resolution of our water sampling (five stations and three water samples per station) introduces some uncertainties into our interpretations, we speculate that salt-induced coagulation of colloidal matter, dissolution/scavenging of lithogenic particles and brine rejection during sea ice formation significantly influence the distribution of REEs throughout the water column in the EGSL.

5.4. Nd isotope signatures of bulk sediment leachates and estuarine waters in the EGSL: Quantifying lithogenic sources

Along continental margins, the dissolved Nd load can be altered by processes such as partial dissolution of river-borne particulate material (e.g., Frank, 2002; Goldstein and Hemming, 2003; Jeandel et al., 2007; Pearce et al., 2013; Jeandel, 2016; Stewart et al., 2016), submarine groundwater discharge (Molina-Kescher et al., 2018), and benthic exchange processes (Abbott et al., 2016; Haley et al., 2017). Furthermore, most of the dissolved Nd within the water column precipitates to form oxyhydroxides in estuarine sediments (Goldstein and Jacobsen, 1988; Elderfield et al., 1990; Ingri et al., 2000; Rousseau et al., 2015). In the EGSL, the overall high agreement between the εNd values from bulk sediment leachates and their corresponding detrital εNd values ($r = 0.88$; $n = 10$; Figs. 8C and 9) supports the idea that variations in authigenic Nd isotopic compositions result mainly from changes in the partial dissolution of riverine detrital particulate material derived from the Grenvillian and Appalachian provinces. Note that sample inhomogeneity combined with unwanted chemical extraction of other phases during sequential leaching may be the cause of the variability in the εNd (±2σ) values in the bulk sediment leachates (e.g., Rutberg et al., 2000; Gutjahr et al., 2007; Haley et al., 2008). Alternatively, the release of REEs from pore waters that are derived from partial dissolution of bottom sediments could also contribute to the offset observed between the εNd signal of surface leached sediments and detrital signatures (Abbott et al., 2016; Haley et al., 2017).

Taking into consideration the detrital εNd endmember values of the Grenville Province and Appalachian Province and assuming a conservative binary mixing, we estimate that the εNd values of dissolved Nd in the estuarine water of the EGSL reflect a mixture of approximately 74% Nd derived from the Canadian Shield and 26% Nd derived from the Appalachian domain (Fig. 10). These results are in agreement with other estimates from EGSL sediments based on bulk mineralogical data, which show a dominance of the sediment contributions from the North Shore in the EGSL (Jaegle, 2015). However, we cannot preclude the possibility that the LCW/NACW εNd signatures also contribute to our authigenic εNd signal (Fig. 9). Given the high river discharges and detrital influence in the EGSL, we hypothesize that the LCW/NACW signal recorded in the EGSL bottom sediments is masked by the detrital εNd signatures of continental river inputs. Consequently, dissolved Nd inputs from the EGSL to North Atlantic surface waters may thus contribute an unradiogenic Nd isotopic composition to the NACW.

Furthermore, the authigenic εNd values obtained from surface sediment leachates closest to the North Shore (COR0602-043BC, COR1004-CE-BC, COR0503-HONOI-14BC, and COR0602-045BC) have an unradiogenic εNd signature that can be obtained by a mixture of 83% Nd inputs from the Grenville Province and 17% Nd inputs from the Appalachian domain (Fig. 10). In contrast, the surface sediment leachates from the shelves (HU2003–033-30PC, COR0503-CL03-35BC, COR1004-ECL-BC, COR0902-16BC, and COR1002-27BC) have more radiogenic εNd values composed of approximately 64% Nd inputs derived from the weathering of the Appalachian Province and 36% Nd inputs derived from the Grenville domain (Fig. 10). Therefore, the authigenic εNd values of the bulk sediment leachates in the EGSL cannot be used to track water mass provenance and mixing but instead reflect the composition of the surrounding continental margins. This interpretation is in agreement with the consideration that dissolved water mass εNd signatures are set at the continental margins, where they would not trace water mass mixing (e.g., Frank, 2002; Jeandel et al., 2007; Rousseau et al., 2015; Stewart et al., 2016).

6. Summary and conclusion

We determined the REE distributions and Nd and Sr isotope compositions on a set of surface marine sediments and at five hydrological stations in the EGSL and continental shelf off southeastern Canada. The (La/Yb)n and (Gd/Yb)n ratios and the εNd and $^{87}Sr/^{86}Sr$ isotope values of detrital sediments allowed the discrimination of continental sediment sources. Modern surface sediments from the continental shelf and Baie des Chaleurs have εNd values ranging from −14.3 to −16.0, $^{87}Sr/^{86}Sr$ values ranging from 0.72708 to 0.71475 and low (La/Yb)n and (Gd/Yb)n values mainly derived from the Appalachian domain. In contrast, surface sediments from the Laurentian-Esquiman channels [εNd = −18.7 to −21.8; $^{87}Sr/^{86}Sr$ = 0.72607 to 0.72068; high (La/Yb)n and (Gd/Yb)n] principally originate from the Grenville Province, and surface sediments from the southern Labrador Shelf [εNd = −28.7; $^{87}Sr/^{86}Sr$ = 0.73062; high (La/Yb)n and (Gd/Yb)n] are likely derived from the Hudson Strait and Baffin Bay. Furthermore, both the estuarine waters (εNd values ranging from −18.9 to −21.7) and the bulk sediment leachates (εNd values ranging from −16.1 to −27.2) have unradiogenic εNd values. The REE distributions and HREE/LREE - εNd crossplots suggest that the authigenic εNd signal recorded in the EGSL results mainly from the erosion and weathering of the unradiogenic continental shield, notably the Grenville Province in the Canadian

Shield (εNd ≈ −22). Overall, both the dissolved REE concentrations and Nd isotope distributions suggest that the distribution of REEs throughout the water column in the EGSL is probably influenced by salt-induced coagulation of colloidal matter, dissolution of lithogenic sediments (notably from the erosion of the Grenville Province on the North Shore), bottom scavenging within the nepheloid layer, and brine rejection during sea ice formation.

Based on the comparison of the εNd values of leached and detrital core-top samples to those of bottom water samples, we hypothesize that the LCW/NACW signal recorded in the EGSL bottom sediments is masked by the lithogenic εNd signals derived from river input. Consequently, the Nd isotope compositions extracted from bulk sediment leachates from the EGSL mainly represent unradiogenic εNd detrital signals from the adjacent continents.

This study provides a basis for comparing downcore εNd, $^{87}Sr/^{86}Sr$, (La/Yb)n, and (Gd/Yb)n values preserved in the EGSL sedimentary records in order to reconstruct and document past variations in continental inputs and sediment dispersal related to climate changes, particularly during the last glacial cycle when sediment inputs would have been different from those of today due to the presence of the Laurentide Ice Sheet.

Supplementary data to this article can be found online at https://doi.org/10.1016/j.marchem.2019.03.012.

Acknowledgments

This research was funded by the *Fonds de recherche du Québec – Nature et technologies* (New university researchers start up program to J.-C. Montero-Serrano), ISMER excellence scholarships (M. Casse), and the Natural Sciences and Engineering Research Council of Canada (NSERC) through Discovery Grants to J.-C. Montero-Serrano and G. St-Onge. We thank the captain, crew, and scientists of the COR0503 and COR0602, COR0902, COR1002, and COR1004 campaigns on board the R/V Coriolis II. We also thank Quentin Beauvais (ISMER), Pascal Guillot (Québec-Océan) and Joël Chassé (IML) for their technical support and advice. Finally, thanks to: Christine Laurin, Thomas Barbour and American Journal Experts for reviewing the grammar; the three anonymous reviewers for their constructive reviews, which improve the quality of the manuscript; and Thomas Bianchi and Alexandra Rao for their editorial work. All analytical data presented are available electronically in the Supplementary Appendix (Tables S4 to S7).

References

Abbott, A.N., Haley, B.A., McManus, J., 2016. The impact of sedimentary coatings on the diagenetic Nd flux. Earth Planet. Sci. Lett. 449, 217–227. https://doi.org/10.1016/j.epsl.2016.06.001.

Adebayo, S.B., Cui, M., Hong, T., White, C.D., Martin, E.E., Johannesson, K.H., 2018. Rare earth elements geochemistry and Nd isotopes in the Mississippi River and Gulf of Mexico mixing zone. Front. Mar. Sci. 5, 166. https://doi.org/10.3389/fmars.2018.00166.

Armstrong-Altrin, J.S., Nagarajan, R., Madhavaraju, J., Rosalez-Hoz, L., Lee, Y.I., Balaram, V., Cruz-Martínez, A., Avila-Ramírez, G., 2013. Geochemistry of the Jurassic and upper cretaceous shales from the Molango region, Hidalgo, eastern Mexico: implications for source-area weathering, provenance, and tectonic setting. Compt. Rendus Geosci. 345 (4), 185–202.

Armstrong-Altrin, J.S., Lee, Y.I., Kasper-Zubillaga, J.J., Trejo-Ramírez, E., 2016. Mineralogy and geochemistry of sands along the Manzanillo and El Carrizal beach areas, southern Mexico: implications for palaeoweathering, provenance and tectonic setting: geochemistry of Beach Sands from Southern Mexico. Geol. J. 57, 1446–1461.

Asahara, Y., Takeuchi, F., Nagashima, K., Harada, N., Yamamoto, K., Oguri, K., Tadai, O., 2012. Provenance of terrigenous detritus of the surface sediments in the Bering and Chukchi seas as derived from Sr and Nd isotopes: implications for recent climate change in the Arctic regions. Deep-Sea Res. II Top. Stud. Oceanogr. 61, 155–171. https://doi.org/10.1016/j.dsr2.2011.12.004.

Barletta, F., St-Onge, G., Stoner, J.S., Lajeunesse, P., Locat, J., 2010. A high-resolution Holocene paleomagnetic secular variation and relative paleointensity stack from eastern Canada. Earth Planet. Sci. Lett. 298 (1), 162–174. https://doi.org/10.1016/j.epsl.2010.07.038.

Bayon, G., German, C.R., Burton, K.W., Nesbitt, R.W., Rogers, N., 2004. Sedimentary Fe–Mn oxyhydroxides as paleoceanographic archives and the role of aeolian flux in regulating oceanic dissolved REE. Earth Planet. Sci. Lett. 224 (3), 477–492. https://doi.org/10.1016/j.epsl.2004.05.033.

Bayon, G., Henderson, G.M., Etoubleau, J., Caprais, J.-C., Ruffine, L., Marsset, T., Dennielou, B., Cauquil, E., Voisset, M., Sultan, N., 2015. U-Th isotope constraints on gas hydrate and pockmark dynamics at the Niger delta margin. Mar. Geol. 370, 87–98. https://doi.org/10.1016/j.margeo.2015.10.012.

Broecker, W.S., Peng, T.-H., 1982. Tracers in the sea. In: Lamont-Doherty Geological Observatory. 1982. pp. 690 Palisades, NY.

Bugden, G.L., 1991. Changes in the temperature-salinity characteristics of the deeper waters of the Gulf of St. Lawrence over the past several decades. Can. Spec. Publ. Fish. Aquat. Sci. 113, 139–147.

Casse, M., 2018. Reconstitution de la variabilité naturelle climatique et océanographique dans l'estuaire et le golfe du Saint-Laurent au cours des 10,000 dernières années. Université du Québec à Rimouski, Institut des sciences de la mer de Rimouski, Thèse. Rimouski, Québec 285 p.

Casse, M., Montero-Serrano, J.-C., St-Onge, G., 2017. Influence of the Laurentide ice sheet and relative sea-level changes on sediment dynamics in the estuary and gulf of St. Lawrence since the last deglaciation. Boreas. https://doi.org/10.1111/bor.12230.

Chen, T.-Y., Frank, M., Haley, B.A., Gutjahr, M., Spielhagen, R.F., 2012. Variations of North Atlantic inflow to the Central Arctic Ocean over the last 14 million years inferred from hafnium and neodymium isotopes. Earth Planet. Sci. Lett. 353, 82–92. https://doi.org/10.1016/j.epsl.2012.08.012.

Crocket, K.C., Hill, E., Abell, R.E., Johnson, C., Gary, S.F., Brand, T., Hathorne, E.C., 2018. Rare earth element distribution in the NE Atlantic: evidence for benthic sources, longevity of the seawater signal, and biogeochemical cycling. Front. Mar. Sci. 5, 147. https://doi.org/10.3389/fmars.2018.00147.

Culshaw, N., Brown, T., Reynolds, P.H., Ketchum, J.W., 2000. Kanairiktok shear zone: the boundary between the Paleoproterozoic Makkovik Province and the Archean Nain Province, Labrador, Canada. Can. J. Earth Sci. 37 (9), 1245–1257. https://doi.org/10.1139/e00-035.

D'Anglejan, B.F., Smith, E.C., 1973. Distribution, transport, and composition of suspended matter in the St. Lawrence estuary. Can. J. Earth Sci. 10, 1380–1396.

van de Flierdt, T., Pahnke, K., Amakawa, H., Andersson, P., Basak, C., Coles, B., Colin, C., Crocket, K., Frank, M., Frank, N., Goldstein, S.L., Goswami, V., Haley, B.A., Hathorne, E.C., Hemming, S.R., Henderson, G.M., Jeandel, C., Jones, K., Kreissig, K., Lacan, F., Lambelet, M., Martin, E.E., Newkirk, D.R., Obata, H., Pena, L., Piotrowski, A.M., Pradoux, C., Scher, H.D., Schöberg, H., Singh, S.K., Stichel, T., Tazoe, H., Vance, D., Yang, J., 2012. GEOTRACES intercalibration of neodymium isotopes and rare earth element concentrations in seawater and suspended particles. Part 1: reproducibility of results for the international intercomparison: Intercalibration of seawater Nd isotopes. Limnol. Oceanogr. Methods 10 (4), 234–251. https://doi.org/10.4319/lom.2012.10.234.

van de Flierdt, T., Griffiths, A.M., Lambelet, M., Little, S.H., Stichel, T., Wilson, D.J., 2016. Neodymium in the oceans: a global database, a regional comparison and implications for palaeoceanographic research. Philos. Trans. R. Soc. A Math. Phys. Eng. Sci. 374 (2081), 20150293. https://doi.org/10.1098/rsta.2015.0293.

De Vernal, A., St-Onge, G., Gilbert, D., 2011. Oceanography and quaternary geology of the St. Lawrence estuary and the Saguenay Fjord. IOP Conference Series: Earth and Environmental Science 14 (1), 012004. https://doi.org/10.1088/1755-1315/14/1/012004.

Dickin, A.P., 2000. Crustal formation in the Grenville Province: Nd-isotope evidence. Can. J. Earth Sci. 37 (2–3), 165–181.

Drinkwater, K.F., 1996. Climate and oceanographic variability in the Northwest Atlantic during the 1980s and early-1990s. J. Northwest Atl. Fish. Sci. 18, 77–97.

Du, J., Haley, B.A., Mix, A.C., 2016. Neodymium isotopes in authigenic phases, bottom waters and detrital sediments in the Gulf of Alaska and their implications for paleocirculation reconstruction. Geochim. Cosmochim. Acta 193, 14–35.

Dufour, R., Ouellet, P., 2007. Estuary and Gulf of St. Lawrence marine ecosystem overview and assessment report. In: Canadian Technical Report of Fisheries and Aquatic Sciences. vol. 112.

Ebbestad, J.O.R., Tapanila, L., 2005. Non-predatory borings in Phanerotrema (Gastropoda), early Silurian, Anticosti Island, Québec, Canada. Palaeogeogr. Palaeoclimatol. Palaeoecol. 221 (3), 325–341. https://doi.org/10.1016/j.palaeo.2005.03.003.

Eberl, D.D., 2003. User Guide to RockJock-A Program for Determining Quantitative Mineralogy from X-Ray Diffraction Data. US Geological Survey, pp. 03–78 Open-File Rep.

Eberl, D.D., Smith, D.B., 2009. Mineralogy of soils from two continental-scale transects across the United States and Canada and its relation to soil geochemistry and climate. Appl. Geochem. 24 (8), 1394–1404.

El Meknassi, S., Dera, G., Cardone, T., De Rafélis, M., Brahmi, C., Chavagnac, V., 2018. Sr isotope ratios of modern carbonate shells: Good and bad news for chemostratigraphy. Geology 46 (11), 1003–1006. https://doi.org/10.1130/G45380.1.

Elderfield, H., Upstill-Goddard, R., Sholkovitz, E.R., 1990. The rare earth elements in rivers, estuaries, and coastal seas and their significance to the composition of ocean waters. Geochim. Cosmochim. Acta 54 (4), 971–991.

Fagel, N., Hillaire-Marcel, C., 2006a. Glacial/interglacial instabilities of the Western boundary under current during the last 365 kyr from Sm/Nd ratios of the sedimentary clay-size fractions at ODP site 646 (Labrador Sea). Mar. Geol. 232 (1), 87–99.

Fagel, N., Hillaire-Marcel, C., 2006b. Glacial/interglacial instabilities of the Western Boundary UnderCurrent during the last 360 kyr from Sm/Nd signatures of sedimentary clay fractions at ODP-Site 646 (Labrador Sea). Mar. Geol. 232, 87–99.

Fagel, N., Innocent, C., Stevenson, R.K., Hillaire-Marcel, C., 1999. Deep circulation changes in the Labrador Sea since the last glacial maximum: new constraints from Sm-Nd data on sediments. Paleoceanography 14 (6), 777–788.

Farmer, G.L., Barber, D., Andrews, J., 2003. Provenance of late quaternary ice-proximal sediments in the North Atlantic: Nd, Sr and Pb isotopic evidence. Earth Planet. Sci.

Lett. 209 (1–2), 227–243.
Filippova, A., Frank, M., Kienast, M., Rickli, J., Hathorne, E., Yashayaev, I.M., Pahnke, K., 2017. Water mass circulation and weathering inputs in the Labrador Sea based on coupled Hf–Nd isotope compositions and rare earth element distributions. Geochim. Cosmochim. Acta 199, 164–184. https://doi.org/10.1016/j.gca.2016.11.024.
Frank, M., 2002. Radiogenic isotopes: tracers of past ocean circulation and erosional input. Rev. Geophys. 40 (1).
Freslon, N., Bayon, G., Toucanne, S., Bermell, S., Bollinger, C., Chéron, S., Etoubleau, J., Germain, Y., Khripounoff, A., Ponzevera, E., Rouget, M.-L., 2014. Rare earth elements and neodymium isotopes in sedimentary organic matter. Geochim. Cosmochim. Acta 140, 177–198. https://doi.org/10.1016/j.gca.2014.05.016.
Gaillardet, J., Viers, J., Dupre, B., 2003. Trace elements in river waters. In: Dreaver, J.I., Holland, H.D., Turekian, K.K. (Eds.), Treatise on Geochemistry. Surface and Groundwater Weathering and Soils. vol. 5. Elsevier-Pergamon, Oxford, pp. 225–272.
Galbraith, P.S., 2006. Winter water masses in the Gulf of St. Lawrence. Journal of Geophysical Research 111 (6), C06022. https://doi.org/10.1029/2005JC003159.
Galbraith, P.S., Chasse, J., Caverhill, C., Nicot, P., Gilbert, D., Pettigrew, B., Lefaivre, D., Brickman, D., Devine, L., Lafleur, C., 2016. Physical Oceanographic Conditions in the Gulf of St. Lawrence in 2015. In: DFO Canadian Science Advisory Secretariat Research Document 2016/056, (90 pp).
Genovesi, L., de Vernal, A., Thibodeau, B., Hillaire-Marcel, C., Mucci, A., 2011. Recent changes in bottom water oxygenation and temperature in the Gulf of St. Lawrence: micropaleontological and geochemical evidence. Limnol. Oceanogr. 56, 1319–1329.
Gilbert, D., Sundby, B., Gobeil, C., Mucci, A., Tremblay, G.-H., 2005. A seventy-two-year record of diminishing deep-water oxygen in the St. Lawrence estuary: the Northwest Atlantic connection. Limnol. Oceanogr. 50 (5), 1654–1666.
Gilbert, D., Chabot, D., Archambault, P., Rondeau, B., Hébert, S., 2007. Appauvrissement en oxygène dans les eaux profondes du Saint-Laurent marin: causes possibles et impacts écologiques. Le Naturaliste Canadien 131, 67–75.
Goldstein, S.L., Hemming, S.R., 2003. Long-lived isotopic tracers in oceanography, paleoceanography, and ice-sheet dynamics. Treatise on Geochemistry 6 (6), 453–489.
Goldstein, S.J., Jacobsen, S.B., 1988. Rare earth elements in river waters. Earth Planet. Sci. Lett. 89 (1), 35–47.
Gutjahr, M., Frank, M., Stirling, C., Klemm, V., Vandeflierdt, T., Halliday, A., 2007. Reliable extraction of a Deepwater trace metal isotope signal from Fe–Mn oxyhydroxide coatings of marine sediments. Chem. Geol. 242 (3), 351–370. https://doi.org/10.1016/j.chemgeo.2007.03.021.
Haley, B.A., Polyak, L., 2013. Pre-modern Arctic Ocean circulation from surface sediment neodymium isotopes: deep Arctic circulation from Nd isotopes. Geophys. Res. Lett. 40 (5), 893–897. https://doi.org/10.1002/grl.50188.
Haley, B.A., Klinkhammer, G.P., McManus, J., 2004. Rare earth elements in pore waters of marine sediments. Geochim. Cosmochim. Acta 68 (6), 1265–1279.
Haley, B.A., Frank, M., Spielhagen, R.F., Fietzke, J., 2008. Radiogenic isotope record of Arctic Ocean circulation and weathering inputs of the past 15 million years: ACEX Pb, Sr, Nd isotope records. Paleoceanography 23 (1). https://doi.org/10.1029/2007PA001486.
Haley, B.A., Du, J., Abbott, A.N., McManus, J., 2017. The impact of benthic processes on rare earth element and neodymium isotope distributions in the oceans. Front. Mar. Sci. 4, 426. https://doi.org/10.3389/fmars.2017.00426.
Hannigan, R.E., Sholkovitz, E.R., 2001. The development of middle rare earth element enrichments in freshwaters: weathering of phosphate minerals. Chem. Geol. 175 (3–4), 495–508.
Henderson, G.M., Martel, D.J., O'Nions, R.K., Shackleton, N.J., 1994. Evolution of seawater $^{87}Sr/^{86}Sr$ over the last 400 ka: the absence of glacial/interglacial cycles. Earth Planet. Sci. Lett. 128 (3–4), 643–651. https://doi.org/10.1016/0012-821X(94)90176-7.
Hodell, D.A., Mead, G.A., Mueller, P.A., 1990. Variation in the strontium isotopic composition of seawater (8 ma to present) : implications for chemical weathering rates and dissolved fluxes to the oceans. Chemical Geology 80 (4), 291–307.
Hollings, P., Stevenson, R., Meng, X., Hillaire-Marcel, C., 2008. Impact of melting of the Laurentide ice sheet on sediments from the upper continental slope off southeastern Canada: evidence from Sm-Nd isotopes. Can. J. Earth Sci. 45 (11), 1243–1252.
Ingri, J., Widerlund, A., Land, M., Gustafsson, Ö., Andersson, P., Öhlander, B., 2000. Temporal variations in the fractionation of the rare earth elements in a boreal river; the role of colloidal particles. Chem. Geol. 166 (1–2), 23–45.
Innocent, C., Fagel, N., Stevenson, R.K., Hillaire-Marcel, C., 1997. Sm-Nd signature of modern and late quaternary sediments from the Northwest North Atlantic: implications for deep current changes since the last glacial maximum. Earth Planet. Sci. Lett. 146 (3–4), 607–625.
Jacobsen, S.B., Wasserburg, G.J., 1980. Sm-Nd isotopic evolution of chondrites. Earth Planet. Sci. Lett. 50 (1), 139–155.
Jaegle, M., 2015. Nature et origine des sédiments de surface de l'estuaire du Saint-Laurent. M.Sc. thesis. Université du Québec à Rimouski (83 pp).
Jeandel, C., 2016. Overview of the mechanisms that could explain the 'boundary exchange' at the Land–ocean contact. Phil. Trans. R. Soc. A 374 (2081), 20150287. https://doi.org/10.1098/rsta.2015.0287.
Jeandel, C., Thouron, D., Fieux, M., 1998. Concentrations and isotopic compositions of neodymium in the eastern Indian Ocean and Indonesian straits. Geochim. Cosmochim. Acta 62 (15), 2597–2607.
Jeandel, C., Arsouze, T., Lacan, F., Techine, P., Dutay, J., 2007. Isotopic Nd compositions and concentrations of the lithogenic inputs into the ocean: a compilation, with an emphasis on the margins. Chem. Geol. 239 (1–2), 156–164.
Jennings, A.E., Andrews, J.T., Pearce, C., Wilson, L., Olfasdottir, S., 2015. Detrital carbonate peaks on the Labrador shelf, a 13 to 7 ka template for freshwater forcing from the Hudson Strait outlet of the Laurentide ice sheet into the subpolar gyre. Quat. Sci. Rev. 107, 62–80.
Koutitonsky, V.G., Bugden, G.L., 1991. The physical oceanography of the Gulf of St. Lawrence: a review with emphasis on the synoptic variability of the motion. Can. Spec. Publ. Fish. Aquat. Sci. 113, 57–90.
Kraft, S., Frank, M., Hathorne, E.C., Weldeab, S., 2013. Assessment of seawater Nd isotope signatures extracted from foraminiferal shells and authigenic phases of gulf of Guinea sediments. Geochim. Cosmochim. Acta 121, 414–435.
Lacan, F., Jeandel, C., 2004. Neodymium isotopic composition and rare earth element concentrations in the deep and intermediate Nordic seas: constraints on the Iceland Scotland overflow water signature: Iceland Scotland overflow water. Geochem. Geophys. Geosyst. 5 (11).
Lacan, F., Jeandel, C., 2005. Acquisition of the neodymium isotopic composition of the North Atlantic deep water: neodymium isotopic composition. Geochem. Geophys. Geosyst. 6 (12). https://doi.org/10.1029/2005GC000956.
Lacan, F., Tachikawa, K., Jeandel, C., 2012. Neodymium isotopic composition of the oceans: a compilation of seawater data. Chem. Geol. 300, 177–184.
Lambelet, M., van de Flierdt, T., Crocket, K., Rehkämper, M., Kreissig, K., Coles, B., Rijkenberg, M.J.A., Gerringa, L.J.A., de Baar, H.J.W., Steinfeldt, R., 2016. Neodymium isotopic composition and concentration in the western North Atlantic Ocean: results from the GEOTRACES GA02 section. Geochim. Cosmochim. Acta 177, 1–29. https://doi.org/10.1016/j.gca.2015.12.019.
Larouche, P., Boyer-Villemaire, U., 2010. Suspended particulate matter in the St. Lawrence estuary and gulf surface layer and development of a remote sensing algorithm. Estuar. Coast. Shelf Sci. 90, 241–249.
Laukert, G., Frank, M., Bauch, D., Hathorne, E.C., Gutjahr, M., Janout, M., et al., 2017. Transport and transformation of riverine neodymium isotope and rare earth element signatures in high latitude estuaries: a case study from the Laptev Sea. Earth Planet. Sci. Lett. 477, 205–217.
Lawrence, M.G., Kamber, B.S., 2006. The behaviour of the rare earth elements during estuarine mixing-revisited. Mar. Chem. 100, 147–161. https://doi.org/10.1016/j.marchem.2005.11.007.
Lazier, J.R.N., Wright, D.G., 1993. Annual velocity variations in the Labrador current. J. Phys. Oceanogr. 23, 659–678.
Li, C.-F., Guo, J.-H., Yang, Y.-H., Chu, Z.-Y., Wang, X.-C., 2014. Single-step separation scheme and high-precision isotopic ratios analysis of Sr–Nd–Hf in silicate materials. J. Anal. At. Spectrom. 29 (8), 1467.
Loring, D.H., Nota, D.J.G., 1973. Morphology and Sediments of the Gulf of St. Lawrence. vol. 182 Bulletin of the Fisheries Research Board of Canada (147 pp).
Lucotte, M., Hillaire-Marcel, C., Louchouarn, P., 1991. First-order organic-carbon budget in the St-Lawrence lower estuary from C-13 data. Estuar. Coast. Shelf Sci. 32, 297–312.
Mai-Thi, N.-N., St-Onge, G., Tremblay, L., 2017. Contrasting fates of organic matter in locations having different organic matter inputs and bottom water O2 concentrations. Estuar. Coast. Shelf Sci. 198, 63–72.
Merschel, G., Bau, M., Dantas, E.L., 2017. Contrasting impact of organic and inorganic nanoparticles and colloids on the behavior of particle-reactive elements in tropical estuaries: an experimental study. Geochim. Cosmochim. Acta 197, 1–13.
Meyer, I., Davies, G.R., Stuut, J.-B.W., 2011. Grain size control on Sr-Nd isotope provenance studies and impact on paleoclimate reconstructions: an example from deep-sea sediments offshore NW Africa: grain size control on Sr-Nd isotope. Geochem. Geophys. Geosyst. 12 (3). https://doi.org/10.1029/2010GC003355.
Millot, R., Gaillardet, J., Dupré, B., Allègre, C.J., 2002. The global control of silicate weathering rates and the coupling with physical erosion: new insights from rivers of the Canadian shield. Earth Planet. Sci. Lett. 196 (1), 83–98.
Molina-Kescher, M., Frank, M., Hathorne, E.C., 2014. Nd and Sr isotope compositions of different phases of surface sediments in the South Pacific: extraction of seawater signatures, boundary exchange, and detrital/dust provenance. Geochem. Geophys. Geosyst. 15 (9), 3502–3520.
Molina-Kescher, M., Hathorne, E. C., Osborne, A. H., Behrens, M. K., Kölling, M., Pahnke, Frank, M., (2018). The influence of basaltic islands on the oceanic REE distribution: a case study from the tropical South Pacific. Front. Mar. Sci., 5. https://doi.org/10.3389/fmars.2018.00050.
Montero-Serrano, J.C., Bout-Roumazeilles, V., Tribovillard, N., Sionneau, T., Riboulleau, A., Bory, A., Flower, B., 2009. Sedimentary evidence of deglacial megafloods in the northern Gulf of Mexico (Pigmy Basin). Quat. Sci. Rev. 28 (27), 3333–3347.
Muzuka, A.N.N., Hillaire-Marcel, C., 1999. Burial rates of organic matter along the eastern Canadian margin and stable isotope constraints on its origin and diagenetic evolution. Mar. Geol. 160, 251–270.
Namur, O., Charlier, B., Toplis, M.J., Higgins, M.D., Liégeois, J.-P., Auwera, J.V., 2010. Crystallization sequence and magma chamber processes in the Ferrobasaltic Sept Iles layered intrusion, Canada. J. Petrol. 51 (6), 1203–1236. https://doi.org/10.1093/petrology/egq016.
Normandeau, A., Lajeunesse, P., St-Onge, G., Bourgault, D., Drouin, S.S.-O., Senneville, S., Bélanger, S., 2014. Morphodynamics in sediment-starved inner-shelf submarine canyons (lower St. Lawrence estuary, eastern Canada). Mar. Geol. 357, 243–255.
Osborne, A.H., Haley, B., Hathorne, E.C., Flögel, S., Frank, M., 2014. Neodymium isotopes and concentrations in Caribbean seawater: tracing water mass mixing and continental input in a semi-enclosed ocean basin. Earth Planet. Sci. Lett. 406, 174–186.
Osborne, A.H., Haley, B.A., Hathorne, E.C., Plancherel, Y., Frank, M., 2015. Rare earth element distribution in Caribbean seawater: continental inputs versus lateral transport of distinct REE compositions in subsurface water masses. Mar. Chem. 177, 172–183.
Palmer, M.R., Elderfield, H., 1985. Sr isotope composition of sea water over the past 75 Myr. Nature 314 (6011), 526–528. https://doi.org/10.1038/314526a0.
Pearce, C.R., Jones, M.T., Oelkers, E.H., Pradoux, C., Jeandel, C., 2013. The effect of particulate dissolution on the neodymium(Nd) isotope and rare earth element (REE) composition of seawater. Earth Planet. Sci. Lett. 369, 138–147.

Petrie, B., Anderson, C., 1983. Circulation on the newfoundland continental shelf. Atmosphere-Ocean 21 (2), 207–226. https://doi.org/10.1080/07055900.1983.9649165.
Phan, T.T., Gardiner, J.B., Capo, R.C., Stewart, B.W., 2018. Geochemical and multi-isotopic (87Sr/86Sr, 143Nd/144Nd, 238U/235U) perspectives of sediment sources, depositional conditions, and diagenesis of the Marcellus shale, Appalachian Basin, USA. Geochim. Cosmochim. Acta 222, 187–211.
Piepgras, D.J., Jacobsen, S.B., 1992. The behavior of rare earth elements in seawater: precise determination of variations in the North Pacific water column. Geochim. Cosmochim. Acta 56 (5), 1851–1862.
Piepgras, D.J., Wasserburg, G.J., 1987. Rare earth element transport in the western North Atlantic inferred from Nd isotopic observations. Geochim. Cosmochim. Acta 51 (5), 1257–1271.
Pinet, N., Brake, V., Campbell, C., Duchesne, M., 2011. Seafloor and shallow subsurface of the St. Lawrence River estuary. Geosci. Can. 38 (1).
Piotrowski, J.A., Larsen, N.K., Junge, F.W., 2004. Reflections on soft subglacial beds as a mosaic of deforming and stable spots. Quat. Sci. Rev. 23 (9), 993–1000. https://doi.org/10.1016/j.quascirev.2004.01.006.
Piper, D.J.W., Mudie, P.J., Fader, G.B., Josenhans, H.W., MacLean, B., Vilks, G., 1990. Quaternary geology. In: Keen, M.J., Williams, G.L. (Eds.), Geology of the Continental Margin of Eastern Canada. Geology of Canada, Series 2 *Geological Survey of Canada*, Ottawa ON, pp. 475–607.
Porcelli, D., Andersson, P.S., Baskaran, M., Frank, M., Björk, G., Semiletov, I., 2009. The distribution of neodymium isotopes in Arctic Ocean basins. Geochim. Cosmochim. Acta 73 (9), 2645–2659. https://doi.org/10.1016/j.gca.2008.11.046.
Portier, A.M., 2015. Sediment Provenance in the Gulf of Mexico: ATest of the Regolith Hypothesis. Master thesis. University of Florida (66 p).
Poulton, S.W., Raiswell, R., 2005. Chemical and physical characteristics of iron oxides in riverine and glacial meltwater sediments. Chem. Geol. 218, 203–221.
Pourmand, A., Dauphas, N., Ireland, T.J., 2012. A novel extraction chromatography and MC-ICP-MS technique for rapid analysis of REE, Sc and Y: revising CI-chondrite and post-Archean Australian shale (PAAS) abundances. Chem. Geol. 291, 38–54.
Pourret, O., Tuduri, J., 2017. Continental shelves as potential resource of rare earth elements. Sci. Rep. 7, 5857. https://doi.org/10.1038/s41598-017-06380-z.
Pratte, S., De Vleeschouwer, F., Garneau, M., 2017. Geochemical characterization (REE, Nd and Pb isotopes) of atmospheric mineral dust deposited in two maritime peat bogs from the St. Lawrence north shore (eastern Canada). J. Quat. Sci. 32, 617–627.
Rashid, H., Saint-Ange, F., Barber, D.C., Smith, M.E., Devalia, N., 2012. Fine scale sediment structure and geochemical signature between eastern and western North Atlantic during Heinrich events 1 and 2. Quat. Sci. Rev. 46, 136–150.
Revel, M., Sinko, J.A., Grousset, F.E., Biscaye, P.E., 1996. Sr and Nd isotopes as tracers of North Atlantic lithic particles: Paleoclimatic implications. Paleoceanography 11 (1), 95–113. https://doi.org/10.1029/95PA03199.
Révillon, S., Hureau-Mazaudier, D., 2009. Improvements in digestion protocols for trace element and isotope determinations in stream and lake sediment reference materials (JSd-1, JSd-2, JSd-3, JLk-1 and LKSD-1). Geostandards & Geoanalytical Research 33, 397–413.
Rousseau, T.C., Sonke, J.E., Chmeleff, J., Van Beek, P., Souhaut, M., Boaventura, G., et al., 2015. Rapid neodymium release to marine waters from lithogenic sediments in the Amazon estuary. Nat. Commun. 6, 7592. https://doi.org/10.1038/ncomms8592.
Rutberg, R.L., Hemming, S.R., Goldstein, S.L., 2000. Reduced North Atlantic deep water flux to the glacial Southern Ocean inferred from neodymium isotope ratios. Nature 405, 935–938.
Saucier, F.J., 2003. Modeling the formation and circulation processes of water masses and sea ice in the Gulf of St. Lawrence, Canada. J. Geophys. Res. 108 (C8). https://doi.org/10.1029/2000JC000686.
Schlitzer, R., 2017. Ocean data view. http://odv.awi.de.
Shabani, M.B., Akagi, T., Masuda, A., 1992. Preconcentration of trace rare-earth elements in seawater by complexation with bis (2-ethylhexyl) hydrogen phosphate and 2-ethylhexyl dihydrogen phosphate adsorbed on a C18 cartridge and determination by inductively coupled plasma mass spectrometry. Anal. Chem. 64 (7), 737–743.
Sheng, J., 2001. Dynamics of a buoyancy-driven coastal jet: the Gaspe current. J. Phys. Oceanogr. 31 (11), 3146–3162.
Sholkovitz, E.R., 1993. The geochemistry of rare-earth elements in the Amazon River estuary. Geochim. Cosmochim. Acta 57, 2181–2190.
Sholkovitz, E.R., 1995. The aquatic chemistry of rare earth elements in rivers and estuaries. Aquat. Geochem. 1, 1–34. https://doi.org/10.1007/BF01025229.
Sholkovitz, E., Szymczak, R., 2000. The estuarine chemistry of rare earth elements: comparison of the Amazon, Fly, Sepik and the Gulf of Papua systems. Earth Planet. Sci. Lett. 179 (2), 299–309. https://doi.org/10.1016/S0012-821X(00)00112-6.
Smith, J.N., Schafer, C.T., 1999. Sedimentation, bioturbation, and hg uptake in the sediments of the estuary and gulf of St. Lawrence. Limnol. Oceanogr. 44, 207–219.
Spivack, A.J., Wasserburg, G., 1988. Neodymium isotopic composition of the Mediterranean outflow and the eastern North Atlantic. Geochim. Cosmochim. Acta 52 (12), 2767–2773.
Stevenson, R., Pearce, C.R., Rosa, E., Hélie, J.-F., Hillaire-Marcel, C., 2018. Weathering processes, catchment geology and river management impacts on radiogenic (87Sr/86Sr) and stable (δ88/86Sr) strontium isotope compositions of Canadian boreal rivers. Chem. Geol. 486, 50–60.
Stewart, J.A., Gutjahr, M., James, R.H., Anand, P., Wilson, P.A., 2016. Influence of the Amazon River on the Nd isotope composition of deep water in the western equatorial Atlantic during the Oligocene–Miocene transition. Earth Planet. Sci. Lett. 454, 132–141.
St-Onge, G., Stoner, J.S., Hillaire-Marcel, C., 2003. Holocene paleomagnetic records from the St. Lawrence estuary, eastern Canada: centennial- to millennial-scale geomagnetic modulation of cosmogenic isotopes. Earth Planet. Sci. Lett. 209 (1–2), 113–130.
St-Onge, G., Duchesne, M.J., Lajeunesse, P., 2011. Marine geology of the St. Lawrence estuary. IOP Conference Series 14, 012003.
Stordal, M.C., Wasserburg, G.J., 1986. Neodymium isotopic study of Baffin Bay water: sources of REE from very old terranes. Earth Planet. Sci. Lett. 77 (3), 259–272.
Syvitski, J.P.M., Silverberg, N., Ouellet, G., Asprey, K.W., 1983. First observations of benthos and seston from a submersible in the lower St. Lawrence estuary. Géog. Phys. Quatern. 37, 227–240.
Tachikawa, K., 2003. Neodymium budget in the modern ocean and paleo-oceanographic implications. J. Geophys. Res. 108 (C8).
Tachikawa, K., Jeandel, C., Vangriesheim, A., Dupré, B., 1999. Distribution of rare earth elements and neodymium isotopes in suspended particles of the tropical Atlantic Ocean (EUMELI site). Deep-Sea Res. I Oceanogr. Res. Pap. 46 (5), 733–755.
Tang, C.L., 1980. Mixing and circulation in the northwestern gulf of St. Lawrence: a study of a buoyancy-driven current system. J. Geophys. Res. 85 (C5), 2787.
Taylor, S.R., McLennan, S.M., 1985. The Continental Crust: Its Composition and Evolution. Blackwell Scientific Publication, Carlton (312 p).
Thibodeau, B., De Vernal, A., Hillaire-Marcel, C., Mucci, A., 2010. Twentieth century warming in deep waters of the Gulf of St. Lawrence: a unique feature of the last millennium: St. Lawrence deep waters warming. Geophys. Res. Lett. 37 (17).
Thibodeau, B., de Vernal, A., Limoges, A., 2013. Low oxygen events in the Laurentian Channel during the Holocene. Mar. Geol. 346, 183–191. https://doi.org/10.1016/j.margeo.2013.08.004.
Trites, R.W., 1972. The Gulf of St. Lawrence from a pollution point of view. In: Ruivo, M. (Ed.), Marine Pollution and Sea Life. FAO Fishing News Books, London, pp. 59–72.
Vinciguerra, V., Stevenson, R., Pedneault, K., Poirier, A., Hélie, J.-F., Widory, D., 2016. Strontium isotope characterization of wines from Quebec, Canada. Food Chemistry 210, 121–128.
Weill, D.F., Drake, M.J., 1973. Europium anomaly in plagioclase feldspar: experimental results and Semiquantitative model. Science 180 (4090), 1059–1060. https://doi.org/10.1126/science.180.4090.1059.
Wilson, D.J., Piotrowski, A.M., Galy, A., Clegg, J.A., 2013. Reactivity of neodymium carriers in deep sea sediments: implications for boundary exchange and paleoceanography. Geochim. Cosmochim. Acta 109, 197–221. https://doi.org/10.1016/j.gca.2013.01.042.
Wu, Q., Colin, C., Liu, Z., Thil, F., Dubois-Dauphin, Q., Frank, N., Tachikawa, K., Bordier, L., Douville, E., 2015. Neodymium isotopic composition in foraminifera and authigenic phases of the South China Sea sediments: implications for the hydrology of the North Pacific Ocean over the past 25 kyr: hydrology of the North Pacific Ocean. Geochem. Geophys. Geosyst. 16 (11), 3883–3904. https://doi.org/10.1002/2015GC005871.
Yashayaev, I., Bersch, M., van Aken, H.M., 2007. Spreading of the Labrador Sea water to the Irminger and Iceland basins. Geophys. Res. Lett. 34, L10602. https://doi.org/10.1029/2006GL028999.
Yeats, P.A., Loring, D.H., 1991. Dissolved and particulate metal distributions in the St. Lawrence estuary. Can. J. Earth Sci. 28, 729–742.
Yeats, P.A., Sundby, B., Bewers, J.M., 1979. Manganese recycling in coastal waters. Mar. Chem. 8 (1), 43–55.
Zhang, J., Nozaki, Y., 1996. Rare earth elements and yttrium in seawater: ICP-MS determinations in the east Caroline, Coral Sea, and South Fiji basins of the western South Pacific Ocean. Geochim. Cosmochim. Acta 60, 4631–4644.